Identification and quantification of particulate tracers of exhaust and non-exhaust vehicle emissions

Aurélie Charron[1,2], Lucie Polo-Rehn[1,2], Jean-Luc Besombes[3], Benjamin Golly[3], Christine Buisson[4], Hervé Chanut[5], Nicolas Marchand[6], Géraldine Guillaud[5], and Jean-Luc Jaffrezo[1]

[1]Univ. Grenoble Alpes, CNRS, IRD, IGE (UMR 5001), F-38000 Grenoble, France
[2]IFSTTAR, F-69675 Bron, France
[3]LCME, Univ. Savoie Mont-Blanc, LCME, F-73000 Chambéry, France
[4]LICIT, ENTPE, IFSTTAR, F-69518 Vaux en Velin, France
[5]Atmo Auvergne-Rhône-Alpes, F-69500 Bron, France
[6]Aix Marseille Univ., CNRS, LCE, F-13331 Marseille, France

Correspondence to: Aurélie Charron (aurelie.charron@univ-grenoble-alpes.fr)

Abstract. In order to identify and quantify key-species associated with non-exhaust emissions and exhaust vehicular emissions, a large comprehensive dataset of particulate species has been obtained thanks to simultaneous near-road and urban background measurements coupled with detailed traffic counts and chassis dynamometer measurements of exhaust emissions of a few in-use vehicles well-represented in the French fleet. Elemental Carbon, brake-wear metals (Cu, Fe, Sb, Sn, Mn), n-alkanes (C19-C26), light molecular weight PAHs (Pyrene, Fluoranthene, Anthracene) and two hopanes (17α21βNorhopane and 17α21βhopane) are strongly associated with the road traffic. Traffic-fleet emission factors have been determined for all of them and are consistent with most recent published equivalent data. When possible, light-duty and heavy-duty duty traffic emission factors are also determined. In absence of significant non-combustion emissions, light-duty traffic emissions are in good agreement with emissions from chassis dynamometer measurements. Since recent measurements in Europe including those from this study are consistent, ratios involving copper (Cu/Fe and Cu/Sn) could be used as brake-wear emissions tracers as long as brakes with Cu remain in use. Near the Grenoble ring road, where the traffic was largely dominated by diesel vehicles in 2011 (70 %), the OC/EC ratio estimated for traffic emissions was around 0.4. Although the use of quantitative data for source apportionment studies is not straightforward for the identified organic molecular markers, their presence seems to well-characterized fresh traffic emissions.

1 Introduction

Traffic is a major source of particulate matter in urban environments through both exhaust and non-exhaust emissions. Thanks to stringent regulations, vehicles with more efficient catalytic converters and diesel particle filters have been progressively introduced into the European fleet. As a consequence particulate exhaust emissions have strongly decreased and non-exhaust particulate emissions (particles resuspended by moving traffic and those from the wear of brakes, tyres, road surface…) will contribute to the major part of particulate vehicular emissions in the near future (Amato et al., 2014). Current research estimates that non-exhaust emissions already substantially contribute to traffic emissions, with differences between sites due to local meteorology, local emissions, or traffic characteristics (e.g. Omstedt et al., 2005; Thorpe and Harrison, 2007; Bukowiecki et al., 2010; Lawrence et al., 2016). Even with electric vehicles, traffic will continue to be a source of PM through non-exhaust emissions (Pant and Harrison, 2013; Timmers and Achten, 2016).

Also, knowledge on the deleterious impacts of PM from vehicular emissions on human health is increasing. There is now strong evidence that traffic-related PM is responsible for adverse health effects due to the health effect of both carbonaceous material from exhaust emissions and redox-active metals in traffic-generated dust including road, brake and tyre wear (Kukutschová et al., 2009; Cassee et al., 2013; Amato et al., 2014 and references wherein; Pardo et al., 2015; Poprac et al., 2017). Recently, on the one hand, Shirmohammadi et al. (2017) and Weber et al., (2018) have shown the important role of non-tailpipe emissions to the oxidative potential of particulate matter species identified as tracers of vehicle abrasion; and on the other hand, the health impacts of coarse particles is now better documented (Beelen et al., 2014; Cheng et al., 2015; Malig et al., 2013). Therefore, a better knowledge on vehicular emissions is required to better understand their contribution to urban atmospheric PM_{10} concentration levels and related health effects.

Chassis dynamometer measurements allow the determination of exhaust vehicular emissions under controlled testing conditions but, because of high costs, these tests often include small sets of vehicles that cannot be representative of large variation in engine type, age and maintenance history of vehicles. They also do not represent the variability of driving types in various environments. All of these are parameters that strongly influence real-world vehicular emissions. Additionally, these tests cannot simulate accurately the effect of dilution on particle equilibrium in the road atmosphere (Kim et al., 2016), the possible rapid aging effects (e.g. Platt et al., 2017), and non-tailpipe emissions (e.g. Thorpe and Harrison, 2008). For all these reasons, it is thought that more realistic estimates of vehicle emissions are determined from air quality measurements in the near-road atmosphere (Phuleria et al., 2017), including car-chasing, tunnel or roadside measurements (Pant and Harrison, 2013 and references therein; Jezek et al., 2015).

In this study, a large comprehensive dataset on the chemical composition of PM_{10} from exhaust and non-exhaust emissions has been obtained thanks to two complementary campaigns: 1) simultaneous near-road and urban background measurements coupled with detailed traffic counts for the estimation of real-world vehicular emissions including non-exhaust emissions and, 2) chassis dynamometer measurements of exhaust emissions of a few in-use vehicles well-represented in the French fleet for the identification of key species in exhaust emissions. This study focuses on PM_{10} in order to take into account for the entire breathable fraction of non-exhaust particulate emissions, a large part of which are coarse particles (Thorpe and Harrison, 2008; Grigoratos and Martini, 2014). Possible particulate tracers of exhaust and non-exhaust vehicle emissions are examined and quantified. Emission factors and when possible, typical ratios, are derived from these data.

2 Methodology

2.1 Chassis dynamometer measurements

Vehicles were operated on a chassis dynamometer, and exhaust emissions were measured using a sampling train including a Constant Volume Sampling (CVS) system in which emissions are diluted with filtered air and sampled using quartz filters and polyurethane foams (PUF).

2.1.1 Vehicle types and driving cycles

Five vehicles representative of the most frequent vehicle classes in the French fleet in circulation were selected (Euro 3 Diesel, Euro 4 diesel, Euro 4 diesel retrofitted with particle filter, Euro 2 petrol, Euro 4 petrol). They were in-use private cars since rental vehicle may not be representative of the national fleet (low mileage). All vehicles

were operated using commercial diesel and petrol fuels. Selection criteria and characteristics of tested vehicles are described in the Supplementary Information (SI).

Driving cycles designed to be representative of real driving conditions in Europe are performed in this study (André, 2004). The ARTEMIS urban cycle represents driving conditions in urban areas (repeated acceleration and vehicle speed below 40 km/h), while the ARTEMIS rural-road cycle represents driving conditions on main roads in suburban and rural areas outside cities (flowing traffic conditions). These cycles represent most driving conditions encountered on the RN87/E712 highway, where the road side experiments took place, during congested and flowing traffic conditions, respectively. Since urban journeys include cold vehicles, the influence of the cold start on urban emissions has been systematically tested.

2.1.2 Exhaust sampling

Vehicles were operated on a chassis dynamometer using a CVS system to dilute exhaust emissions with filtered ambient air. The filtration system included four filters and a cartridge in series: a M6-F7-F9, M5, F7 EN-779-2012 filters; a HEPA H13 EN1822-2009 filter; and a cylindrical cartridge of charcoal scrubber.

Regulated emissions were determined with continuous monitors for CO, CO_2, NO_x, and total hydrocarbons (HORIBA system). Particulate matter (PM) and volatile organic compounds (VOC) were sampled out from the dilution tunnel with a servo-controlled system designed by Serv'Instrument for this study. Two driving cycles in series were performed in order to collect enough matter for molecular speciation. PM was collected on quartz filters (Tissuquartz^{TM}, diameter 47 mm), at flow rates depending on both emission levels of the vehicles being tested and the types of analyses (from 5 to 50 L.min^{-1} for EC/OC measurements and from 30 to 50 L.min^{-1} for organic molecular speciation). Dilution factors ranged from about 15 to 40. Conditions of vehicle tests are detailed in the supplemental section (Table I-2). Filter face velocities for chassis dynamometer samplings dedicated to organic speciation were similar or close to the one of atmospheric near-road measurements, while, because of very high concentration levels, lower sample flow rates are used for PM samplings dedicated to EC and OC measurements in the exhaust of diesel vehicles non-retrofitted with Particulate Filter (Euro 3 and Euro 4 diesel vehicles). These very low filter velocities may influence the adsorption of organic vapours by the Quartz filter (McDow and Huntzicker, 1990; Turpin et al., 2000 ; Vecchi et al., 2009), while EC would not be affected by filter face velocity (Vecchi et al., 2009). Quartz filters were pre-baked at 500°C for 8h before being used. Samples were stored at -18°C in aluminum foil and sealed in polyethylene bags until analyses.

Analysis of test blank filters (collected following the same procedure as vehicle test filters including driving cycle durations with filtered air) showed contaminations from the CVS system. It was obvious that some organic compounds measured in test blanks result from the desorption of semi-volatile organics deposited into the CVS, that is favoured by cleaner air. Since blank levels decreased in time with passing air dilution through the system, our procedure included such a step maintained for a duration corresponding to at least two driving cycles before each vehicle test. Test blanks are used to correct measurements.

2.2 Near-road and urban background measurements

The joint PM-DRIVE (PM-Direct and Indirect on-road Vehicular Emissions) and MOCOPO (Measuring and mOdelling traffic Congestion and POllution) field campaign took place from September 9th to 23rd, 2011. It

included meteorology and traffic measurements, near-road/urban background PM_{10} sampling (this study) and near-road on-line measurements (discussed in DeWitt et al., 2015).

2.2.1 Description of traffic and urban background sites

The Grenoble conurbation is a large city with about 700,000 inhabitants. It is located in the southeast of France in the French Alps and is surrounded by three mountain ranges (Vercors, Chartreuse, and Belledone). The traffic site was located (45.150641 N, 5.726028 E) about 15 m away from the southern part of the Grenoble ring road (the RN87/E712 highway with 2×2 lanes) (26 m from the roadway central axis). Total traffic flow for the 4 lanes was on average 95,000 and 65,000 vehicles a day on workday and weekend, respectively, with frequent congestion during extended commuting hours. Stop-and-go traffic in both directions generates large braking activity at that time. This sampling site was highly equipped during the joint PM-DRIVE / MOCOPO field campaign. Simultaneous measurements took place at an urban background site (Les Fresnes) which is located about 2 km away from the traffic site, on the rooftop of a school. This site belongs to the regional air pollution network managed by Atmo Auvergne-Rhône-Alpes (http://www.atmo-auvergnerhonealpes.fr/). The locations of both sites are presented on Figure 1.

2.2.2 Aerosol and gas measurements

On both traffic and urban background sites, PM_{10} HiVol (DA80, 30 m^3 h^{-1}) samplers collected PM_{10} on quartz fibre filters (Tissuquartz™, diameter 150 mm) with a time resolution of 4 hours. Filters were preheated at 500 °C during 3 h. After sampling, filters were individually placed in aluminum foil, sealed in polyethylene bags and stored at −18 °C until analysis. In addition, both sites were equipped with NO_x (NO and NO_2) and CO monitors. PM_{10} and $PM_{2.5}$ mass concentrations were also continuously measured using 8500C series TEOM-FDMS (Filter Dynamics Measurement System and Tapered Element Oscillating Microbalance mass sensor housed in a single-cabinet compact enclosure).

2.2.3 Traffic measurements

Traffic counters (double electromagnetic loops) were installed in order to identify the passing of all vehicles, the length of their chassis and their speeds, the determination of the 2 vehicle classes used in this study (light-duty and heavy-duty vehicles), and the identification of periods of stop-and-go or flowing traffic. Vehicle mean speeds are computed as the harmonic mean speed of the cars passing over the detector (flow speed i.e. the spatial mean speed) (Hall, 2001).

Traffic cameras mounted on a roadway gantry were also used to monitor traffic at the measurement site. They were used to capture the license plate numbers of passing vehicles. Plate numbers were later used to classify vehicular traffic into different categories: EURO standards and fuel type (diesel or petrol). The traffic of the highway is detailed elsewhere (DeWitt et al., 2015; Fallah Shorshani et al., 2015). On weekdays, the average hourly traffic included 2,850 diesel vehicles (including about 200 heavy-duty vehicles) and 1,025 petrol vehicles. The harmonic vehicle mean speed was about 80 km/h and ranged from 52 to 94 km/h (note that the RN87 highway has a speed limit of 90 km/h). A sample is considered affected by congested traffic above a threshold of more

22,000 vehicles during the 4-h sampling periods (corresponding to vehicle speed below 70 km/h) (see SI file). However, braking may occur below this threshold for congestion.

The vehicle fleet was close to the national one for the year 2011, with 72% diesel vehicles, and EURO 3 and 4 vehicles representing most of the vehicles (30 and 36% respectively). Virtually all heavy-duty vehicles are diesel.

2.2.4 Meteorological measurements

A Young meteorological station was installed at the traffic site to capture wind speed and direction, while relative humidity, and temperature data and rain data are obtained from two stations located in Grenoble conurbation (see SI file section IV).

The wind speed was low during the field campaign (on average 0.98 m/s, ranging from 0.50 to 2.5 m/s). The temperature was warm (on average 17.6°C, peaked to 27°C) and was higher before the first rain event (on Sunday 17/09/11) with average temperatures of 21°C and 15°C, respectively, before and after the rain event. Two rain events occurred during the campaign, the first one from the morning of 17/09/11 to the night of 18/09/11 night (34 mm of rain) and the second one from the night of 18/09 to 19/09/11 afternoon (12.7 mm). They corresponded to summer storms.

2.3 Chemical analyses

The measurements of carbonaceous material (EC and OC) in PM samples were performed using the Thermo-Optical Transmission (TOT) method on a Sunset Lab analyser (Jaffrezo et al., 2005; Aymoz et al., 2006) following the EUSAAR2 temperature protocol (Cavalli et al., 2010). Ionic species were analyzed with Ionic Chromatography (IC) following a well-established method (Jaffrezo et al., 1998; Waked et al., 2014). Metals were analyzed using Inductively Coupled Plasma Spectrometry (ICP-MS) (Waked et al., 2014). The chemical speciation of organic particles are performed by Gas Chromatography–Mass Spectrometry (GC-MS), except PAHs that were measured by liquid chromatography (HPLC) using a fluorescence detector (Piot, 2011; Golly et al., 2015).

Hence, a large number of particulate chemical species have been measured in the filter samples simultaneously collected at the traffic and urban background sites, including EC, OC, 9 major ions (Cl^-, NO_3^-, SO_4^{2-}, oxalate, Na^+, NH_4^+, K^+, Mg^{2+}, Ca^{2+}), 33 metals and trace elements (Al, As, Ba, Ca, Cd, Ce, Co, Cr, Cs, Cu, Fe, K, La, Li, Mg, Mn, Mo, Na, Ni, Pb, Pd, Pt, Rb, Sb, Sc, Se, Sn, Sr, Ti, Tl, V, Zn, Zr), 3 sugars (galactosan, mannosan, levoglucosan), 15 PAHs (phenanthrene, anthracene, fluoranthene, pyrene, retene, benzo(a)anthracene, chrysene, benzo(e)pyrene, benzo(b)fluoranthene, benzo(k)fluoranthene, benzo(a)pyrene, benzo(ghi)perylene, dibenzo(a,h)anthracene, indeno(1,2,3-cd)pyrene, coronene), 30 n-alkanes (from C10 to C40), 2 branched alkanes (pristane and phytane) and 10 hopanes (trisnorneohopane, 17α-trisnorneohopane, 17α,21β-norhopane, 17α21β-hopane, 17α,21β,-22S-homohopane, 17α,21β,-22R-homohopane, 17α,21β,-22R-bishomohopane, 17α,21β,-22S-bishomohopane, 17α,21β,-22S-trishomohopane, 17α,21β,-22R-trishomohopane).

The same array of chemical species were also quantified in the filter samples from the chassis dynamometer experiments.

2.4 Data analysis

A series of multivariate data analysis tools have been used in order to define which species are related to traffic, to identify influential parameters, and to quantify their respective influences. Thanks to simultaneous measurements at near-traffic and background sites, local increments in concentration at the traffic site have been calculated as the difference between near-traffic and urban background concentrations. Sign and Rank Signed-Wilcoxon tests have been used to estimate if concentrations measured at the near-traffic site are significantly higher than concentrations measured at the urban background site and can possibly be ascribed to local traffic emissions. As a complementary indication of relation to traffic, Spearman correlations with traffic data (total traffic, light-duty traffic, heavy-duty traffic), with NO_x (as an indicator of traffic emissions) and with EC (as an indicator of diesel traffic emissions) (Morawska and Zhang, 2002; Reche et al., 2011) have also been examined. Results for species for which concentrations are significantly higher at the near-traffic site (then including both positive increments and p-values below 0.05 from Sign and Signed Wilcoxon tests) are presented in Tables 1a and 1b.

Increments in concentrations for all species strongly associated with traffic are transformed into emissions according to a well-established procedure (e.g. Pant and Harrison, 2013; Charron and Harrison, 2005; details in the SI section V). This method enables the calculation of average emission factors for the mixed traffic fleet of the RN87 highway assuming that (1) increments in concentration (near-traffic site minus urban traffic site) are from local traffic, (2) emissions of NO_x are known and estimated from emission inventories (COPCETE that uses emission functions from European COPERT4 averaged for fleet composition and speed) and detailed traffic counts and (3) atmospheric dilution affects similarly all pollutants. Average emission factors (EFs) are expressed in $mg.veh^{-1}.km^{-1}$ or $\mu g.veh^{-1}.km^{-1}$ (Tables 2a,b,c,d). Since it is thought that nearby industrial activities influence the concentrations of Ti, Cr, Fe and Mn in the morning, these data are excluded from the calculations. Standard multiple Linear Regression analyses (SPSS software) are performed between computed average emission data and light-duty and heavy-duty vehicle counts. The coefficients of the regressions represent average EFs for local heavy-duty and light duty traffics (Table 3). The constants represent the parts not related to local traffic. They are all not significant (p-values above 0.4 for metals and organics, p-value of 0.061 for EC) confirming the above assumption that mostly local traffic contributes to local increments in concentration. Results from Multiple Linear Regressions are not available for all species strongly related to traffic since its use requires normally-distributed data and the model must be validated through residues analyses.

3 Results

Average concentrations measured at the traffic site are presented in the SI (section II). Four-hour PM_{10} concentrations ranged from 4.9 to 45.1 $\mu g.m^{-3}$ (on average 24.1 $\mu g.m^{-3}$) and was strongly dominated by EC (on average 5.9 $\mu g.m^{-3}$) and OC (on average 5.4 $\mu g.m^{-3}$). At this site in the vicinity of traffic dominated by diesel vehicles, EC and OC concentrations were of similar magnitude. EC concentrations peaked at commuting time in the early morning and at the end of the afternoon, and follows quite well the evolution of traffic; the temporal evolution of OC is closer to that of sulphate with somewhat stronger variability following those of traffic. The other major constituents of PM_{10} were sulphate (on average 1.2 $\mu g.m^{-3}$), iron (on average 1.0 $\mu g.m^{-3}$) and calcium (on average 0.8 $\mu g.m^{-3}$). Strong showers during the weekend in the middle of the two-week campaign led to PM_{10} concentrations below 10 $\mu g/m^3$during a few hours (see Figure 3 and SI VII for individual particulate species).

3.1 Identification of species related to local on-road traffic

Tables 1a and 1b present species for which concentrations are significantly higher at the near-traffic site and assumed from local emissions and Figure X present median concentrations measured at both sites. These species could be distributed into two main groups according to both the significance of the contribution of traffic to atmospheric levels and the strength of relations with traffic indicators (traffic counts, NO_x and EC concentrations).

3.1.1 Species strongly associated with local traffic

Cu, Fe, Mn, Sb, Sn have concentrations strongly correlated with traffic indicators (Table 1a). Their local increments in concentration due to traffic range from 54% to 84%. The concentrations of these species are linearly related to each other with near-zero intercepts (Figure 4) confirming that they come from the same source. Similarly to this study, Amato et al. (2011a) and Harrison et al. (2012) measured strong increments for Fe, Cu, Sb and Sn concentrations at traffic sites with strong correlations between them. Here, Cu, Fe and Sn are the metals that are the most closely related (Pearson $r^2 \geq 0.8$), while relationships with Mn and Sb are more scattered (Pearson $r^2 < 0.5$) and more closely related to the heavy-duty traffic (Table 1a).

Cr and Ti are also species significantly correlated to traffic indicators but to a lower extent than Cu, Fe, Mn, Sb and Sn. Cr (Boogaard et al., 2011 ; Amato et al., 2011a) and Ti (Amato et al., 2011a) also showed higher atmospheric concentrations at street locations than at urban background sites in previous studies. Cr and Ti show a behaviour different from that of other elements coming from brake wear. They present sharp peaks in the morning, poorer correlations with copper, and significant correlations with Al (Figure 4 and Table 1a). When the very high morning concentrations are removed (mornings of workdays), their temporal variations are much closer to the ones of metals from brake wear emissions. This suggests that another source influenced Cr and Ti concentrations near the traffic site in the morning, possibly nearby metalworking activities. Similarly, while morning peaks are less obvious in the temporal variations, the exclusion of morning data for Fe and Mn improves their correlations with Cu (Figure 4).

Many of these species are metals that are known to arise from brake wear emissions (Thorpe and Harrison, 2008; Pant and Harrison, 2013; Grigoratos and Martini, 2014, 2015). Indeed, Fe could come from the lining (steel or iron powder) in semi-metallic brake, from fibres as steel, or cast iron rotor wear for low metallic brake. Cu is a high-temperature lubricant present in linings and it is also included in fibres as brass to increase braking performance. Sb is an element of brake lining both in filler as antimony sulphate and in lubricant as antimony trisulphide. Chromium oxides are elements of the filler of brake linings used for their thermal properties, and potassium titanate fibers are present as a strengthener in organic linings (Sanders et al., 2003; Grigoratos and Martini, 2014 and references therein). Cr could also come from lubricant oil combustion (Pulles et al., 2012).

Only three light molecular weight PAHs (An, Fla, Pyr) are strongly associated with traffic indicators even though only the particulate phase is determined (Table 1b). It is well-established that light molecular weight PAHs are emitted by diesel vehicles, while higher molecular weight PAHs are rather associated with petrol vehicle emissions (Zielinska et al., 2004; Phuleria et al., 2006 and 2007; Pant and Harrison, 2013). Not surprisingly, in this site dominated by diesel vehicles, high molecular weight PAHs (from 5 rings) are more significantly correlated with levoglucosan, suggesting a closest relation to biomass burning emissions than to on-road petrol vehicles. Proportional concentrations of An, Pyr, and Fla suggest that they mainly come from the same source, likely diesel exhaust emissions (Figures 3 and 4). Specifically, Pyr and Fla show high increments in concentration (as an indication of the low contribution of the urban background compared to strong traffic contribution, and/or rapid

photochemical degradation) and strong linear relationship without any significant intercept (as an indication of common origin). Concentrations of An have more variability and larger contribution from the urban background.

The n-alkanes C19 to C26 and two hopanes (17α21βnorhopane and 17α21βhopane) are species that are not significantly, or only weakly, correlated to total traffic. However, they are significantly correlated with NO_x and EC and some of them with heavy-duty traffic. The n-alkanes between C18 and C25 are the predominant ones in vehicle exhaust and correspond to the high boiling point components in diesel fuels (Alves et al., 2016). Hopanes are known to arise from unburnt lubricating oil emissions (Rogge et al. 1993a; Zielinska et al., 2004), and 17α21nNorhopane is considered as a tracer for lubricating oil (Kleeman et al., 2008). While n-alkanes have been measured in the exhaust of test diesel vehicles in our study (Table 4), hopanes and steranes were below the quantification limit for all selected vehicles. It was assumed that the tested vehicles (passenger cars, none of them was a super-emitting vehicle) did not emit enough unburnt oil for the proper quantification of hopanes. At the sampling site, the temporal variations of the concentrations of these species show higher values on the second week of the field campaign than on the first one. This observation can be explained by much larger heavy-duty traffic during this period (almost twice the traffic of the first week).

3.1.2 Other species

This second group corresponds to species with local increments below 50% and no significant, or only weak, correlations with traffic indicators. It is highly heterogeneous since it includes OC, NO_3^-, Na^+, Ca^{2+}, Mg^{2+}, Ba, Co, Phenanthrene (Phe), Benzo(a)Anthracene (BaA) and some n-alkanes (C18, and from C27 to C33). Most of species from this group are obviously emitted by the traffic but they seem to be less specific than species from the first group since other sources can largely contribute to their emission levels.

Not surprisingly NO_3^- is not significantly related to primary traffic indicators. However its concentrations are significantly higher at the traffic site ($p<0.001$, and median increment of 28%). Additionally, the temporal pattern of NO_3^- is different from that of indicators of regional origin (for example SO_4^{2-}, SI section VII). Amato et al. (2011a) found similar contributions of traffic to NO_3^- concentrations at two traffic sites in Barcelona (34% and 25% respectively). They assumed that NH_4NO_3 is quickly formed in the road plume enriched in NH_3 emitted by vehicles. Indeed, the important introduction of vehicles equipped with DeNOx technology such as 3-way catalysts or selective catalytic reduction systems have led to recent increasing vehicular NH_3 emissions (Kean et al., 2009; Suarez-Bertoa and Astorga, 2016) responsible for significant changes in the chemistry of the atmosphere in roadside areas.

OC concentrations are significantly higher at the traffic site ($p<0.001$; increment of 23%), and are weakly but significantly correlated with traffic indicators. Amato et al., (2011a) found slightly higher increments of 34% and 41% for OC at their 2 traffic sites. Deconvolution of sources from simultaneous PM_1 AMS measurements concluded that about 20% of the total PM_1 organic mass could be attributed to vehicular emissions (DeWitt et al., 2015). Additionally, the temporal pattern of OC concentrations clearly shows a dominant regional contribution (Figure 3 and SI section VII). All these results agree that in summer time, the majority of OC is of regional origin, despite a clear influence of traffic.

Na^+, Ca^{2+}, Mg^{2+} and Sr concentrations are also significantly higher at the traffic site ($p<0.05$, increments from 33% to 43%, except for Sr for which urban background concentrations are most of the time below detection limit). When three high concentrations for Mg^{2+} concentrations and one for Sr concentration are excluded (all probably

not related to traffic), both present temporal variations close that of calcium (Figure 3). All are at least significantly correlated to the heavy-duty traffic ($p<0.05$). Since Ca^{2+}, Mg^{2+} and Sr are strongly affected by rain events (assumed to influence the silt loading of the road), their incremental concentrations are believed to be from resuspended dust, as concluded in other studies (e.g. Lough et al., 2005, Amato al., 2011a).

Ba and Co concentrations are significantly higher at the traffic site ($p<0.05$, increments of 37% and 36% respectively). Ba concentrations present a temporal behaviour close to the ones of Cu, Fe, Sn and Mn and, accordingly, is known as an element of the filler of brake linings. Higher Ba atmospheric concentrations at street locations than at urban background sites have also been observed in previous studies (Harrison et al., 2012). On the contrary, Co concentrations do not show any correlation with traffic indicators and are correlated with tracers of regional origin (Table 1a). Co is sometimes measured in brake pads (e.g. Hulskotte et al., 2014); and Amato et al. (2011) found similar increments for Co at their traffic sites (respectively 33% and 47%). All of these suggest that a possible contribution of brake wear to Co concentrations cannot be excluded, despite the lack of correlation with traffic indicators.

The concentrations of Phe, BaA, C18 and C27-C33 alkanes are significantly higher at the traffic site and some of them are significantly correlated with NO_x and EC. Accordingly these species were detected in the exhaust emissions of diesel vehicles sampled from our chassis dynamometer experiments. However most of them are also significantly correlated with levoglucosan measured at the traffic site, particularly BaA. Indeed the temporal pattern of BaA shows similarities with both the one of Pyr (strongly related to traffic, see below) and levoglugosan (tracer of biomass burning peaking in the evening) (Figure 3). It is therefore believed that most of them are largely emitted by biomass burning and are not specific of road traffic emissions.

3.2 Quantification of traffic fleet emissions for species associated with traffic

Average emission factors (EFs) are presented in Tables 2a,b,c,d. Most EFs show large standard deviations. This variability reflects the presence of vehicles with various emission levels (diesel/petrol; different standards and engine load; cold start/hot vehicles; presence of a few high emitting vehicles). It could also be related to the variability of the vehicle fleet (on-average 5% heavy vehicles but ranging from 0.3% to 12%) and to the various traffic conditions (from fluid with speeds up to 90 km/h to congested with stop-and-go traffic).

Table 3 presents average EFs for heavy-duty and light duty traffics, their standard deviations and confidence intervals at 95%.

3.2.1 EC/OC emissions

The traffic-fleet EF for EC determined in this study (39 $mg.veh^{-1}.km^{-1}$) is slightly higher than the ones determined in tunnel studies in Austria, China, California, and near a heavily-trafficked highway in Switzerland (about 21 $mg.veh^{-1}.km^{-1}$ for Handler et al., 2008; Hueglin et al., 2006; Cui et al., 2016; and 31 $mg.veh^{-1}.km^{-1}$ for Gillies et al., 2001), while it is similar to the one of a tunnel study in Portugal (39 $mg.veh^{-1}.km^{-1}$) (Alves et al., 2015). Conversely, the traffic-fleet EFs for OC in Austria and China (about 19 $mg.veh^{-1}.km^{-1}$) are similar to ours, while the ones for urban tunnels in Portugal (Alves et al., 2015) and U.S. (Gillies et al., 2001) are higher (39 $mg.veh^{-1}.km^{-1}$ and 25 $mg.veh^{-1}.km^{-1}$ respectively). Different traffic fleet and traffic conditions may explain these small divergences. Part of the differences may also be due to the different measurement techniques used for the distinction between EC and OC.

The average light-duty traffic-fleet EF for EC is in excellent agreement with the EFs of Euro 3 and Euro 4 diesel vehicles obtained from chassis dynamometer measurements in our study for which the highest EFs were clearly observed when vehicles are cold (Figure 5a). Indeed, these two types of vehicles represented the largest proportion of passenger's cars on the RN87 freeway in 2011 (Fallah Shorshani et al., 2015), as well as in the French national fleet. Similarly to results for diesel vehicles tested by Fujita et al. (2007) and Lough et al. (2007), EC has the highest emission factor in diesel exhaust. It also could be noted that the heavy-duty traffic-fleet EF for EC is about 5-times higher than the one determined for light-duty traffic.

The emissions of OC could not be discriminated between light-duty and heavy-duty traffic (coefficients not significantly different from zero). However, it can be observed that the traffic-fleet EF for OC is larger than could be expected from exhaust measurement of test vehicles (Table 4, Figure 5b). Note that traffic-fleet EFs for OC from other studies (Handler et al., 2008; Alves et al., 2015, Cui et al., 2016; He et al., 2008) are at least as high as ours, and the EFs for exhaust OC from Cheung et al. (2010) for Euro 4 diesel vehicles (with and without Diesel Particulate Filter) is similar to ours. There are many likely explanations for the traffic-fleet EF for OC being higher than expected: proportionally larger contribution of the heavy-duty traffic to OC than to the EC; contribution of non-exhaust emissions to the OC (e.g. tyres wear); contribution of high emitting vehicles; and rapid formation of secondary OC in the roadside atmosphere. Further studies are required to assess the respective importance of these processes. In particular, a better knowledge of particle size distribution of OC emitted by traffic might be useful.

Average OC/EC ratios on increments in concentrations and emissions are respectively 0.33 and 0.44 (Table 5) that is in excellent agreement with observations in a roadway tunnel in Lisbon and with roadside enrichment of OC/EC in Birmingham, U.K. (Pio et al., 2011; Alves et al., 2016). Pio et al. concluded that OC/EC ratios of 0.3-0.4 characterizes vehicle fuel combustion at their sites and similar conclusions could be made for Grenoble. However, the OC/EC ratio is expected to depend on vehicle fleet. Indeed, in the exhaust of test diesel vehicles without particle filters (Table 4), OC/EC ratios are lower than 0.4, while they are respectively 6.1 and 1.7 in the exhaust of Euro 2 petrol vehicle (urban cold cycle) and Euro 4 petrol vehicle (road cycle) (no average OC/EC ratios has been determined for petrol vehicles because of many measurements below detection limit). Other recent chassis dynamometer measurements (Lough et al., 2007) showed that most OC/EC ratios are above 2 for petrol vehicles (except for two smoker vehicles) and below 0.5 for diesel vehicles (except idling conditions), with even lower ratios for older and heavier diesel vehicles. Because in 2011, diesel vehicles represented about 70% of total vehicles on the RN87 highway, the OC/EC ratio found in this study is lower than the ones of many other studies. For examples, OC/EC ratios from EFs or increments in concentrations were 0.90±0.21 in a tunnel in Austria (Handler et al., 2008); on average 0.52 for a traffic fleet with 40% diesel vehicles in Spain (Amato et al., 2011a) and 0.5 in Marseille where petrol two-wheelers are much more numerous (El Haddad et al., 2009). However, since the OC/EC ratio in the exhaust of the diesel vehicle equipped with particle filter was higher (0.7) possibly due to the more efficient trapping of EC than OC by the particle filter, one can expect that in the future the OC/EC ratio reflecting vehicle fuel combustion would increase with the progressive introduction of vehicles equipped with PF.

3.2.2 Metals from brake wear emissions

Fe presents by far the third highest traffic emission rate after those of EC and OC (6.7 mg.veh^{-1}.km^{-1}, Tables 2). Cu also shows a high emission factor from traffic (300 µg. veh^{-1}.km^{-1} respectively). Similarly, major contributions of Fe and Cu to PM_{10} vehicular emissions were found in other locations (e.g. Kam et al., 2012; Harrison et al.,

2012). The analysis of brake wear debris (Apeagyei et al., 2011 ; Sanders et al., 2003 ; Kukutschová et al., 2009 ; Hulskotte et al., 2014) and brake material (Gigoratos and Martin, 2015; Hulskotte et al., 2014) confirmed that Fe is the major element of brakes and that Cu is another important element. Indeed, maximum contents of 60% by mass for Fe (Gigoratos and Martin, 2015) and of 15% for Cu (Denier van der Gon et al., 2007) have been reported for brake lining materials. Fe, Cu, Zn, Sn would represent about 80-90% of metals presents in brake pads and Fe 95% of metals in brake discs (Hulskotte et al., 2014)

Our results can be compared with other European traffic EFs determined for PM_{10} species measured in roadside environments or tunnels, and with data derived from average brake wear composition (details in SI, section VIII). Most PM_{10}-EFs are consistent with other roadside traffic fleet emissions (Johansson et al., 2009; Bukowiecki et al., 2009) and with data corresponding to braking emissions of 8 $mg.veh^{-1}.km^{-1}$ (Hulskotte et al. 2014), but larger than the estimations aimed to quantify brake wear only (Bukowiecki et al., 2009). Our traffic-fleet EF for Sb is much lower than similar EFs determined in other studies, while Ba emissions show large variability from a study to another. EFs related to brake wear component emissions are lower in tunnel environments (Handler et al., 2008; Alves et al., 2015), except for the oldest study (Gillies et al., 2001). This could be explained by less stop and go traffic in such environments. Indeed, interestingly, many EFs determined by Handler et al. (2008) are about half the ones found in this study. Even though this proportionality is not found for Ba, Sb and Ti, this supports that brake wear metal EFs are strongly related with braking strength. The low Sb emissions of our study may possibly be related to the introduction of Sb-free brake pads (von Uexküll et al., 2005; Apeagyei et al., 2011).

EFs for brake wear metals (Cu, Fe, Sb and Sn) are 8 to 13 times higher for the heavy-duty traffic than for the light-duty traffic (Table 3). The estimations from Bukowiecki et al. (2009) for brake wear only are much lower than ours but somewhat proportional (factors 4.6 to 6.8 for light-duty EFs and from 4.3 to 8.5 for the heavy-duty traffic – Sb excluded). This consistence between brake profiles suggests that brake compositions would be similar in different European countries. Traffic-fleet light-duty EFs for brake wear metals are much higher than the ones from chassis dynamometer exhaust measurements (this study: Table 4; Cheung et al., 2010), confirming the dominant contribution of braking for these elements.

The sum of traffic-fleet EFs for metals related to brake wear (Ba, Cr, Cu, Fe, Mn, Sb, Sn, Ti - Table 2b) leads to a total of 7.3 mg/km that should be lower than the real emission factors for brake wear dusts since it only includes metals, and does not take into account of carbonaceous material and other unquantified compounds of brakes (S, Zn, Al, and Si, for the most important ones). Hulskotte et al. (2014) determined a brake profile from the analysis of 65 brake pads and 15 brake discs from 8 very common car brands in Europe. The consistence between with their data and ours suggests that brakes spent in France are quite similar to the ones spent in The Netherlands. Then, their average brake profile data are used to estimate the average emission factor for brake wear assuming that the total proportion of metals is kept, and, according to Hulskotte et al., that 70% of the wear arise from the disc. This latter assumption is supported by other researches (Sander et al., 2003; Varrica et al., 2013), even though the generation mechanisms of brake wear particles have not been fully understood yet (Grigoratos and Martini, 2014). Since exhaust emissions (chassis dynamometer measurements or EFs from COPCETE inventory when available) represent less than 5% of total emissions for Cr, Cu, Fe, Mn, Sb, Sn, and Ti, traffic-fleet EFs for these elements are assumed to be entirely due to the emissions of brake wear dusts. So by adding to the sum of traffic-fleet EFs for metals related to brake wear the portion that corresponds to the elements and compounds not quantified in this study (C, S, Zn, Al, Si, Zr, Mo, V, Ni, Bi, W, P, Pb, Co), the rough estimation of 9.2 mg/km for

emissions related to brake wear is got for the RN87 highway traffic. This estimation includes particles directly emitted during braking and those resuspended, and emissions from light and heavy-duty traffic. It should be highlighted that this EF for brake wear emissions is almost twice the particle emission standards for the exhausts of the most recent vehicles (Euro 5 and Euro 6 vehicles, 5 mg/km).

According to inventories atmospheric copper is largely from brake wear. Indeed brake wear represents 50-75% of European Cu emissions (Denier Van der Gon et al., 2007) and 64% of French Cu emissions (CITEPA, 2018). Since Sb is another well-known constituent of brake with very few other atmospheric sources, Cu/Sb ratio was often considered as a candidate to trace brake wear emissions (Gietl et al., 2010; Pant and Harrison, 2013). Pant and Harrison (2013) reviewed Cu/Sb ratios in brake wear particles and found ratios from 1.3 to 9.1 that strongly depend on the PM size fraction. The estimation for the Cu/Sb ratio (11.7±5.1 for incremental PM_{10}) is close to the ones for PM_{10} elemental concentrations in other European locations including London, U.K. (on average 9.1, Gietl et al., 2010), Barcelona, Spain (7.0-7.9, Amato et al., 2011a); Bern and Zurich, Switzerland (respectively 13.2 and 8.5, Hueglin et al., 2005) and in road dust below 10 µm collected in Barcelona, Zürich and Girona (respectively 6.8±0.9, 13.5±6.1, 17.0±8.9, Amato et al., 2011). However, lower PM_{10} Cu/Sb ratio are found for other European traffic sites, in Sweden (4.6±2.3, Sternbeck et al., 2002 and 3.8, Johansson et al., 2009); in Portugal (about 2, Alves et al., 2015) and in Vienna, Austria (1.6, Handler et al., 2008). To complicate the matter further, published data from the analysis of brake pads and discs are even more scattered, roughly from 1.3 to 2000 (Adachi et al., 2004; Canepari et al., 2008; Ijima et al., 2007), and often different than the chemical composition of brake wear particles (Grigoratos and Martini, 2015). The poorer relationship between Cu and Sb (Pearson r^2= 0.4) than those observed between Sn, Cu and Fe (Pearson r^2>0.8) and the lower EF for Sb of this study than observations at other sites may be explained by the introduction of Sb-free brake pads. Thus, while the occurrence of Sb may be largely explained by braking activities, the use of a typical factor for braking activities using Sb seems to be less obvious.

The very strong linear relationships found between Fe, Cu, Mn and Sn with no significant intercept (virtually equal to zero) suggests that ratios including these compounds also worth attention. Even though Fe is much less specific of brake wear emissions than Cu or Sb, Hulskotte et al. (2014) observed a stable Cu/Fe ratio of about 4 % in different European kerbside locations (The Netherlands: Boogaard et al., 2011; England: Gietl et al., 2010; Switzerland: Hueglin et al., 2005). They concluded that brake wear is probably the single source of both copper and iron in urban aerosols. The review of other recent studies leads to similar conclusions. Pio et al. (2013) determined an average Fe/Cu ratio of 21 (and then, Cu/Fe = 0.048) from tunnel and busy roads measurements in Portugal. Cu/Fe ratios at two traffic sites in Barcelona ranged from 0.034 to 0.058 (Amato et al., 2011a). Except for the site of Weerdsingel in Utrecht, Cu/Fe ratios calculated from average PM_{10} elemental concentrations measured at 8 street locations in The Netherlands also ranged from 0.039 to 0.048 (Boogaard et al., 2015). Only Alves et al. (2015) found a much higher Cu/Fe ratio in PM_{10} collected in a tunnel in Portugal mainly due to a very low EF for Cu compared to other studies. The Cu/Fe ratio determined in our study for light-duty traffic (0.041±0.010) is very similar to the ones found in the majority of these European roadside sites (Table 5), while the ratio determined for the heavy-duty traffic (0.070±0.017) is slightly larger due to proportionally higher emissions of Cu. Again, this suggests that brake materials used in different European countries are very similar and that the Cu/Fe ratio could be used as an indication of brake wear emissions.

Ratios with Mn and Sn are more rarely discussed in the literature, and published information is scarce. Cu/Sn ratios of 6.2 and 4.3 can be calculated from data published by Handler et al. (2008) and Johansson et al. (2009),

respectively. Amato et al. (2011a) found Cu/Sn ratio that ranged from 4.7 to 4.8 and did not estimate ratios with Mn because of the possible influence of a local steel source. Cu/Mn ratios of 3.7; 4.9 and 3.0 (Bern) and 4.4 (Zurich) are respectively calculated from the studies of Handler et al. (2008), Johansson et al. (2009), and Hueglin et al. (2005). All these ratios are close to the ones of this study (Cu/Sn=4.1±1.0; Cu/Mn=3.6±1.6, Table 5), showing that they are possible other candidates to trace brake wear emissions. Cu/Sn would be the strongest candidate since the relation between these 2 elements is closer (r^2=0.84 for Cu/Sn vs. r^2=0.47 for Cu/Mn, see SI).

3.2.3 Emissions of organic markers of diesel exhaust and lubricating oil

As previously observed (Schauer et al., 2002; Perrone et al., 2014; El Haddad et al., 2009), n-alkanes are abundant organic compounds of total quantified organic compounds emitted by vehicles on road.

In agreement with other chassis dynamometer measurements (Rogge et al.; 1993a; Cheung et al., 2010; Perrone et al., 2014; Cui et al., 2017), the most important n-alkanes in diesel exhaust emissions are C19 to C26, while, most emissions were below detection limit for the two petrol vehicles (Table 4). Schauer et al. (2002) showed that n-alkanes are present in particulate exhaust emissions of non-catalyst equipped petrol vehicles, but they are almost absent in the exhaust of catalyst-equipped petrol motor vehicles. In 2011 virtually all petrol vehicles were catalyst-equipped (Fallah Shorshani et al., 2015). C19-C26 n-alkanes are also the most important in roadside increments in concentration and as a further indication of road traffic contribution, the Carbon Preference Index (CPI, for calculation see SI section VI) is very close to unity (0.99) indicating equal distribution between odd and even carbon number typical of anthropogenic emissions (Harrad et al., 2003; Cincinelli et al., 2007; Kam et al., 2012; Alves et al., 2016). Light-duty traffic-EFs for C23 and C24 are in agreement with the ones of the Euro 3 diesel vehicle from chassis dynamometer measurements (upper range) and with the ones determined by Perrone et al. (2014) for Euro 3 diesel vehicles (C23: 16.3 µg/km ; C24: 12.7 µg/km). Good agreements are also found for C25 and C26. However, the traffic-EFs determined by Perrone et al. for C21 is half the one of this study, the one for C20 is 1/5 of the one of this study. All EFs determined by Perrone et al. for Euro 4 diesel vehicles are larger the ones of the Euro 4 diesel vehicle of this study, but of similar size of magnitude.

The relative contributions of the n-alkane series in diesel exhaust show Gaussian-like shapes peaking between C20 and C22 (Rogge et al.,1993a; Morawska and Zhang, 2002; El Haddad et al.,2009; Cheung et al., 2010; Fujitani et al., 2012; Perrone et al., 2014; Cui et al., 2017). In this study, the dominant alkanes are C21 in the exhaust of test diesel vehicles and C22 in traffic RN87 emissions (Figure 6). Fujitani et al. (2012) showed that shifts from C20 to C22 and differences between real-atmosphere measurements and exhaust measurements are entirely explained by gas-to-particle partitioning at different dilution ratios (dominant n-alkanes were C20 and C22 at dilution ratios of 14 and 238 respectively). Accordingly, in this study, C21 is the dominant n-alkane at diesel exhaust dilution ratios of about 80; and a shift toward a heavier n-alkane has been observed in the roadside atmosphere. N-alkanes normalized by OC (µg/g) (Figure 6) show values for Euro 3 and Euro 4 diesel emissions and RN87 traffic emissions that are about half of the values measured in a tunnel in Marseille (El Haddad et al., 2009). Much higher values are found with the vehicle retrofitted with PF (Figure 6). These high values are due to very low OC emissions by the vehicle equipped with PF and clearly show less effective reduction of n-alkanes than total OC. Because of their semi-volatile nature, n-alkanes may pass the particle filter in their gaseous phase at higher temperatures. While the n-alkanes series from C19 to C26 peaking around C20-C22 seems to be characteristics of diesel emissions, increase of the n-alkane/OC values could be expected for the future.

Low molecular weight PAH's (An, Fla, Pyr) are frequently associated with particulate diesel exhaust emissions (e.g. Kleeman et al., 2008; Keyte et al., 2016). Accordingly, both chassis dynamometer and *in-situ* measurements indicate that diesel vehicles is a major source of these chemical species. Indeed, they are almost absent in petrol exhaust emissions and are strongly related to RN87 traffic emissions. EFs for PAHs determined for the heavy-duty traffic are much higher than the ones determined for light-duty traffic: from 6-times higher for Fla, up to 20-times higher for Pyr (Table 3). High emissions of Pyr by heavy-duty vehicles have already been observed anywhere else (Liacos et al., 2012; Cui et al., 2017). While the comparison between EFs determined during different conditions is not straightforward in absence of gas phase measurements due to the high vapour pressure of the lowest molecular weight organics (Fujitani et al., 2012; Polo Rehn, 2013), quite good agreements are found between chassis dynamometer measurements and traffic-EFs; and with data from other studies. Indeed, again the light-duty traffic-EFs for Fla and Pyr are quite consistent with the ones of the diesel Euro 3 measured with chassis dynamometer. The light-duty traffic-EF for An is proportionally lower, somewhere between the ones of test Euro 3 and Euro 4 vehicles. The average EF for Pyr for the Euro 3 diesel vehicle of this study (Table 4) is close to the ones of Perrone et al. (2014) for Euro 3 diesel vehicles (740±300 ng/km for passenger cars and 1810±570 ng/km for commercial utility vehicles). Traffic EFs for Fla and Pyr are also in good agreement with average EFs in a tunnel in China (40-50 $km.h^{-1}$/784-2776 $veh.h^{-1}$/18.4-35.1% HDV, He et al., 2008). These satisfying agreements suggest that EFs determined in this research may be quite well representative of in-use vehicles. However, gas-particle partitioning and photochemical degradation processes may make difficult the use of quantitative data for these markers, as already observed (Zhang et al., 2005; Phuleria et al., 2007; Katsoyiannis et al., 2011; Tobiszewski and Namieśnik, 2012).

In agreement with previous observations (Phuleria et al., 2006 and 2007; He et al., 2008; El Haddad et al., 2009; Alves et al., 2016; Pant et al., 2017), 17α,21β-norhopane and 17α,21β-hopane are the two dominant hopanes associated with traffic emissions. Very few traffic-EFs are available for hopanes in the recent literature and most data available from recent studies are related to fuel consumption (e.g. Phuleria et al., 2006 and 2007). Traffic hopane EFs of this study are much lower than those computed for tunnels in China (He et al. 2008; Cui et al. 2016). In order to compare with European tunnel data, traffic-EFs are normalized by OC emissions. The normalized abundance of 17α,21β-norhopane (246 µg per g of OC) is similar to the one for a tunnel in Lisbon (Alves et al., 2016) but almost half the ones for tunnels in Marseille and Birmingham (El Haddad et al., 2009; Pant et al., 2017). Conversely, the value for 17α,21β-hopane (301 µg per g of OC) is very close to the ones found in tunnels in Birmingham and Marseille but twice the one for the tunnel in Lisbon. These divergences and the quantification of heavy-duty traffic emissions require further work in order to be able to define specific EFs and normalized abundances for hopanes.

3.2.4 Other non-exhaust emissions

The average traffic-fleet EFs for Ca^{2+} is the fifth highest traffic-fleet emission factor after EC, OC, Fe and NO_3^-. While the emissions of Ca^{2+} could not be discriminated between light-duty and heavy-duty traffics (autocorrelation), this much larger emission factor than the ones measured in the exhaust of diesel vehicles is in agreement with its origin. If Ca^{2+} mainly comes from road dust resuspension, it does not only depend on the intensity of traffic but also on the amounts of calcium deposited on the road (silt loading). Bukowiecki et al. (2009) used the mass concentration measured 1-hour earlier in order to empirically account for the observed

autocorrelation behaviour in the calcium time series due to the accumulation of resuspended dust. The time series resolution of 4 hours for collected particles in this study does not allow such calculations. Note that contrary to Bukowiecki et al., most other trace elements that could be regressed in this study do not have the same behaviour as Ca^{2+}. This could be explained by the removal of road dusts thanks to frequent rain events before and during the sampling period.

Since EU tyres contain about 1% zinc oxide (Pant and Harrison, 2013) and Zn is the most abundant metallic element in tyres commercialized in the U.S. (Apeagyei et al., 2011), Zn is often proposed as a key tracer of tyre wear emissions. In this study, similarly to other works (Boogaard et al., 2011; Amato et al., 2011), Zn concentrations did not show any roadside increment. This suggests the prevalence of other sources of Zn in the Grenoble-Alpes conurbation, as well as in other urban environments. Further research are needed to determine proper tracers of tyre wear emissions.

4. Conclusions

Thanks to a very large comprehensive dataset of particulate species collected from a simultaneous near-road and urban background measurement field campaign and chassis dynamometer experiments of a few in-use passenger cars, this study was able to determine emission factors for many particulate species from road traffic and to identify and quantify tracers of exhaust and non-exhaust vehicular emissions that could be used in source apportionment studies. Near-road measurements are made near a freeway with various driving conditions from free-flowing to stop-and-go traffic, including frequent and severe braking events during periods of congestion (morning and afternoon commuting times of workdays).

EC has the highest traffic emission factors and is strongly associated with diesel traffic. The emission factor for EC for the light-duty traffic is similar to the ones of passenger diesel cars without particle filters. EC emissions from heavy-duty vehicles are estimated to be 5 times higher than those for light duty vehicles. The traffic-fleet EF for OC is slightly larger than those deduced from exhaust measurement of test vehicles. This later observation would require further investigations in order to delineate the several possible causes for such observation. The determination of the particle size distribution of OC could improve knowledge of the organic emissions of traffic. In this environment dominated by the diesel traffic, the OC/EC ratio is below 0.4 (increments in concentration or emissions), as it is in diesel exhaust emissions. However, this ratio depends on the traffic fleet and then may change in the future with the progressive introduction of vehicles retrofitted with particle filter.

Results showed the important contribution of metals from brake wear to particulate vehicular emissions. In particular, Fe has the third higher traffic emission factor after EC and OC. Total brake wear emissions are estimated for the RN87 highway, they are on average almost twice the particle emission standards for the exhausts of newer vehicles (from Euro 5). We have shown that Cu is another important contributor to PM_{10} from traffic and it could be an excellent tracer of brake wear emissions in most environments. Even though they are less specific than Cu, other metals such as Fe and Sn may be used to trace brake wear emissions through typical ratios. In particular, ratios Cu/Fe of about 0.041 for light-duty traffic may possibly be the best option for estimating the brake wear emissions due to the traffic of European passenger cars. Cu/Fe ratios in agreement with literature values for other kerbside sites, while Cu/Fe ratios may be different for urban background or rural sites (e.g. Hueglin et al., 2005; this study: Les Frênes' data), suggest similar brake composition for these elements throughout Europe (as long as Cu-free brakes do not increase in use). Our measurements support more the use of Cu/Sn than that of Cu/Mn and

Cu/Sb as tracers of brake wear emissions possibly due to an additional source of Mn and the introduction of Sb-free brake pads. Similarly to OC, the determination of the particle size distribution of metals may possibly improve the discrimination between influential sources in urban areas.

Particulate organic emission data for European motor vehicles is scarce. In this study, a few PAHs, n-alkanes and hopanes have been identified as organic molecular markers of fresh diesel traffic emissions and their emission factors have been quantified. In agreement with previous works, low molecular weight PAHs (mainly An, Fla, Pyr) are associated with diesel exhaust emissions. Pyrene and Fluoranthene are the ones the most strongly associated with fresh diesel exhaust emissions. Pyrene is more largely emitted by the heavy-duty traffic. Similarly to PAHs, n-alkanes from C19 to C26 are also associated with diesel vehicles, even though the determination of the concentration of the dominant alkanes (from C20 to C23) strongly depends on measurement conditions. While the comparison with other recent studies can be difficult in the absence of gas quantification for *in situ* measurements, a quite good agreement is found for most organics between chassis dynamometer and near-road measurements and between this study and other recent studies. However, the change of the gas-particle partitioning of low molecular PAHs and n-alkanes according to ambient temperature and dilution factors, and their possible short-term photochemical degradation may compromise their use as quantitative markers of fuel combustion.

Hopanes are markers of lubricating oil in the emissions of high-emitting vehicles (Rogge et al. 1993a; Zielinska et al., 2004). In this study two hopanes (17α,21β-norhopane and 17α,21β-hopane) have been clearly associated with the traffic and more closely related to the heavy-duty traffic. However the quantification of ratios hopanes to OC showed divergences with other studies that require a better understanding.

This study determines many quantitative data of traffic exhaust and non-exhaust emissions that could help in a better definition of traffic emissions in source apportionment studies.

Acknowledgements

This work was funded by CORTEA-ADEME (PM-DRIVE program 1162C0002) that includes the funding of chassis dynamometer and near-road field/urban background campaigns and PREDIT (MOCoPo programme) that includes the near-road field measurements of regulated pollutants and traffic characteristics. Lucie Polo-Rehn's PhD was funded by the Région Rhône-Alpes. Rain data was supplied by Météo France. The authors would like to thank Patrick Tassel, Pascal Perret and Mathieu Goriaux (chassis dynamometer experiments), Julie Cozic and Jean-Charles Francony (sample analyses) for their contribution to this work. We also thank Michel André for supplying COPCETE emission factors. Part of the chemical analysis was performed on equipment provided by Labex OSU@2020 (ANR10 LABX56).

References

Adachi K., Tainosho Y.: Characterization of heavy metals particles embedded in tire dust, Environment International 30, pp. 1009-1017, 2004.

Alves C. A., Gomes J., Nunes T., Duarte M., Calvo A., Custodio D., Pio C., Karanasiou A., Querol X.: Size-segregated particulate matter and gaseous emissions from motor vehicles in a road tunnel, Atmospheric Research 153, pp. 134-144, 2015.

Alves C. A.,Oliveira C., Martins N., Mirante F., Caseiro A., Pio C., Matos M., Silva H.F., Oloveira C., Camões F.: Road tunnel, roadside, and urban background measurements of aliphatic compounds in size-segregated particulate matter, Atmospheric research 168, 139-148, 2016.

Amato F., Viana M., Richard A., Furger M., Prévôt A.S.H., Nava S., Lucarelli F., Bukowiecki N., Alastuey A., Reche C., Moreno T., Pandolfi M., Pey J., Querol X.: Size and time-resolved roadside enrichment of atmospheric particulate pollutants, Atmospheric Chemistry and Physics 11, pp. 2917-2931, 2011a.

Amato F., Pandolfi M., Moreno T., Furger M., Pey J., Alastuey A., Bukowiecki N., Prévôt A.S.H., Baltensperger U., Querol X.: Source and variability of inhalable road dust particles in three European cities, Atmospheric Environment 11, pp. 6777-6787, 2011b.

Amato F., Casse F.R., Denier van der Gon H.A.C., Gehrig R., Gustafsson M., Hafner W., Harrison R.M., Jozwicka M., Kelly F.J., Moreno T., Prevot A.S.H., Schaap M., Sunyer J., Querol X.: Urban air quality: The challenge of traffic non-exhaust emissions, Journal of Hazardous Materials 275, 31-36: 2014.

André M.: The ARTEMIS European driving cycles for measuring car pollutant emissions, Sci. Total Environ. 334-335, 73-84, 2004.

André M, Roche A.L., Bourcier L. : Statistiques de parcs et trafic pour le calcul des émissions de polluants des transports routier pour la France. In French. Rapport IFSTTAR LTE, Bron (France), 132pp., 2013.

Apeagyei, E., Bank M. S., Spengler J. D.: Distribution of heavy metals in road dust along an urban-rural gradient in Massachusetts, Atmospheric Environment 45, 2310-2323, 2011.

Aymoz G., Jaffrezo J.-L., Chapuis D., Cozic J., Maenhaut W.: Seasonal variation of PM_{10} main constituents in two valleys of the French Alps I: EC/OC fractions, Atmospheric Chemistry and Physics Discussions 6, 6211-6254, 2006.

Beelen R.; Raaschou-Nielsen O.; Stafoggia M.; Andersen Z. J.; Weinmayr G.; Hoffmann B.; Wolf K.; Samoli E.; Fischer P.;Nieuwenhuijsen M.;Vineis P.;Xun W. W.; Katsouyanni K.; Dimakopoulou K.; Oudin A.; Forsberg B.; Modig L.; Havulinna A. S.; Lanki T.; Turunen A.; Oftedal B.; Nystad W.; Nafstad P.; De Faire U.; Pedersen N. L.; Ostenson C. G.; Fratiglioni L.; Penell J.; Korek M.; Pershagen G.; Eriksen K. T.; Overvad K.; Ellermann T.; Eeftens M.; Peeters P. H.; Meliefste K.; Wang M.; Bueno-de-Mesquita B.; Sugiri D.; Kramer U.; Heinrich J.; de Hoogh K.; Key T.; Peters A.; Hampel R.; Concin H.; Nagel G.; Ineichen A.; Schaffner E.; Probst-Hensch N.; Kunzli N.; Schindler C.; Schikowski T.; Adam M.; Phuleria H.; Vilier A.; Clavel-Chapelon F.; Declercq C.; Grioni S.; Krogh V.; Tsai M. Y.; Ricceri F.; Sacerdot, C.; Galassi C.; Migliore E.; Ranzi A.; Cesaroni G.; Badaloni C.; Forastiere F.; Tamayo I.; Amiano P.; Dorronsoro M.; Katsoulis M.; Trichopoulou A.; Brunekreef B.; Hoek G.,

2014, Effects of long-term exposure to air pollution on natural-cause mortality: an analysis of 22 European cohorts within the multicentre ESCAPE project., Lancet 383, 785-95, doi: 10.1016/s0140-6736(13)62158-3.

Boogaard H., Kos, G.P.A., Weijers E.P., Janssen N. A.H., Fischer P.H., van der Zee S.C., de Hartog J.J., Hoek G.: Contrast in air pollution components between major streets and background locations : Particulate matter mass, black carbon, elemental composition, nitrogen oxide and ultrafine particle number, Atmospheric Environment 45, pp. 650-658, 2011.

Bukowiecki, N., Lienemann P., Hill M., Figi R., Richard A., Furger M., Rickers K., Falkenberg G., Zhao Y., Cliff S.S., Prévôt A.S.H., Baltensperger U., Buchmann B., Gehrig R.: Real-world emission factors for antimony and other brake wear related trace elements: size-segregated values for light and heavy duty vehicles, Environmental Science and Technology 43, 8072-8078, 2009.

Canepari S., Perrino C., Olivieri F., Astolfi M. L.: Characterisation of the traffic sources of PM through size-segregated sampling, sequential leaching and ICP analysis, Atmospheric Environment 42, pp. 8161-8175, 2008.

Cassee F. R., Héroux M.-E., Gerlofs-Nijland M. E., Kelly F. J.: Particulate matter beyond mass: recent health evidence on the role of fractions, chemical constituents and sources of emission, Inhalation Toxicology 25, pp. 802-812, 2013.

Cavalli F., Viana M., Yttri K.E., Genberg J., Putaud J.P.: Toward a standardized thermal-optical protocol for measuring atmospheric organic and elemental carbon: the EUSAAR protocol, Atmos. Meas. Tech 3, 79-89, 2010.

Cheng M. H., Chiu H. F., Yang C.Y., 2015, Coarse particulate air pollution associated with increased risk of hospital admissions for respiratory diseases in a Tropical city, Kaohsiung, Taiwan, International Journal of Environmental Research and Public Health 12, 13053-13068, doi: 10.3390/ijerph121013053.

Cincinelli, A., Del Bubba M., Martellini T., Gambaro A., Lepri L.: Gas-particle concentration and distribution of n-alkanes and polycyclic aromatic hydrocarbons in the atmosphere of Prato (Italy), Chemosphere 68, 472-478, 2007.

CITEPA, édition mars 2018. Inventaire des émissions de polluants atmosphériques en France métropolitaine, format CEE-NU, https://www.citepa.org/images/III-1_Rapports_Inventaires/CEE-NU/UNECE_France_mars2018.pdf

Cui M., Chen Y., Tian C., Zhang F., Yan C., Zheng M.: Chemical composition of $PM_{2.5}$ from two tunnels with different fleet characteristics, Science of the Total Environment 550, 123-132, 2016.

Cui M., Chen Y., Feng Y., Li C., Zheng J., Tian C., Yan C., Zheng M.: Measurement of PM and its chemical composition in real-world emissions from non-road and on-road diesel vehicles, Atmospheric Chemistry and Physics 17, 6779-6795, 2017.

Denier Van der Gon, H.A.C., Hulskotte J.H.J., Visschedijk A.J.H., Schaap M.: A revised estimate of copper emissions from road transport in UNECE Europe and its impact on predicted copper concentrations, Atmospheric Environment 41, pp. 8697-8710, 2007.

DeWitt H.L., Hellebust S., Temime-Roussel B., Ravier S., Polo L., Jacob V., Buisson C., Charron A., André M., Pasquier A., Besombes J.L., Jaffrezo J.L., Wortham H., Marchand N.: Near-highway aerosol and gas-phase measurements in a high-diesel environment, Atmospheric Chemistry and Physics 15, 4373-4387, 2015.

El haddad I., Marchand N., Dron J., Temime-Roussel B., Quivet E., Wortham H., Jaffrezo J.L., Baduel C., Voisin D., Besombes J.L., Gille G.: Comprehensive primary particulate organic characterization of vehicular exhaust emissions in France, Atmosheric Environment 43, 6190-6198, 2009.

Fallah Shorshani M.F., Seigneur C., Polo Rehn L., Chanut H., Pellan Y., Jaffrezo J.L., Charron A., André M.: Atmospheric dispersion modeling near a roadway under calm meteorological conditions, Transportation Research Part D, 34, 137-154, 2015.

Fujita E.M., Zielinska B., Campbell D.E., Arnott W.P., Sagebiel J.C., Mazzoleni L., Chow J.C., Gabele P.A., Crews W., Snow R., Clark N.N., Wayne W.S., Lawson D.R.: Variations in speciated emissions from spark-ignition and compression-ignition motor vehicles in California's south Coast air basin, J. Air Waste Manag. Assoc. 57, 705-720, 2007.

Fujitani Y., Saitoh K., Fushimi A., Takahashi K., Hasegawa S., Tanabe K., Kobayashi S., Furuyama A., Hirano S., Takami A.: Effect of isothermal dilution on emission factors of organic carbon and n-alkanes in the particle and gas phases of diesel exhaust, Atmospheric Environment 59, 389-397, 2012.

Gietl J.K., Lawrence R., Thorpe A.J., Harrison R. M.: Identification of brake wear particles and derivation of a quantitative tracer for brake dust at a major road. Atmospheric Environment 44, 141-146, 2010.

Gillies J.A., Gertler A.W., Sagebiel J.C., Dippel W.A.: On-road particulate matter ($PM_{2.5}$ and PM_{10}) emissions in the Sepulveda tunnel, Los Angeles, California, Environment Science and Technology 35, 1054-1063, 2001.

Golly B., Brulfert G., Berlioux G., Jaffrezo J.-L., Besombes J.-L.: Large chemical characterisation of PM_{10} emitted from graphite material production: Application in source apportionment, Science of Total Environment 558, 634-643, 2015.

Grigoratos T. and Martini G.: Brake wear particle emissions: a review, Environ. Sci. Pollut. Res., 22, 2491-2504, 2015.

Hagino H., Oyama M., Sasaki S.: Laboratory testing of airborne brake wear particle emissions using a dynamometer system under urban city driving cycles, Atmospheric environment 131, pp 269-278, 2016.

Hall, F. Chapter 2: Traffic stream characteristics, in Traffic flow theory: A state of the art report, Gartner, N., Messer, C., Rathi, A. Editors, http://www.tft.pdx.edu/docs.htm, accessed July 2014., 2001.

Handler M., Puls C., Zbiral J., Marr I., Puxbaum H., Limbeck A.: Size and composition of particulate emissions from motor vehicles in the Kaisermühlen-Tunnel, Vienna, Atmospheric Environment 42, pp. 2173-2186, 2008.

Harrad S., Hassoun S., Callén Romero M.S., Harrison R.M.: Characterization and source attribution of the semi-volatile organic content of atmospheric particles and associated vapour phase in Birmingham, UK, Atmospheric Environment 37, 4985-4991, 2003.

Harrison R.M., Jones A.M., Gietl J., Yin J., Green D.C.: Estimation of the contributions of brake dust, tire wear, and resuspension to nonexhaust traffic particles derived from atmospheric measurements. Environmental Science and technology 46, 6523-6529, 2012.

Hueglin, C., Gehrig R., Baltensperger, Gysel M., Monn C., Vonmont H.: Chemical characterization of $PM_{2.5}$, PM_{10} and coarse particles at urban near-city and rural sites in Switzerland., Atmospheric Environment, 39, 637-651, 2005.

Hueglin C., Buchmann B., Weber R.O.: Long-term observation of real-world road traffic emission factors on a motorway in Switzerland, Atmospheric Environment 40, 3696-3709, 2006.

Hulskotte J.H.J., Roskam G.D., Denier van der Gon H.A.C.: Elemental composition of current automotive braking materials and derived air emission factors, Atmospheric Environment, 99, 436-445, 2014.

Ijima A, Sato K., Yano K., Tago H., Kato M., Kimura H., Furuta N.: Particle size and composition distribution analysis of automotive brake abrasion dusts for the evaluation of antimony sources of airborne particulate matter, Atmospheric Environment 41, pp. 4908-4919, 2007.

Jaffrezo J.L., Calas, N., Bouchet M.: Carboxylic acids measurements with ionic chromatography, Atmos. Environ. 32, 2705-2708, 1998.

Jaffrezo J.L., Aymoz G., Delaval C., Cozic J.: Seasonal variations of the water soluble organic carbon mass fraction of aerosol in two valleys of the French Alps, Atmopheric Chemistry and Physics 5, 2809-2821, 2005.

Jezek I., Katrasnik T., Westerdahl D., Mocnik G., Black carbon, particle number concentration and nitrogen oxide emission factors of random in-use vehicles measured with the on-road chasing method, Atmospheric Chemistry and Physics 15, 11011-11026, 2015.

Johansson C., Norman M., Burman L.: Road traffic emission factors for heavy metals, Atmospheric Environment 13, pp. 4681-4688, 2009.

Kam W., Liacos J. W., Schauer J. J., Delfino R. J., Sioutas C.: On-road emission factors of PM pollutants for light-duty vehicles (LDVs) based on urban street driving conditions, Atmospheric Environment, pp. 378-386, 2012.

Katsoyiannis A., Sweetman A.J., Jones K.C.: PAH molecular diagnostic ratios applied to atmospheric sources: a critical evaluation using two decades of source inventory and air concentration data from the UK, Environmental Science and Technology 45, 8897-8906, 2011.

Kean A.J., Littlejohn D., Ban-Weiss G.A., Harley R.A., Kirchstetter T.W., Lunden M.M.: Trends in on-road vehicle emissions of ammonia, Atmospheric Environment 43, 1565-1570, 2009,

Kim Y., Sartelet K., Seigneur C., Charron A., Besombes J.L., Jaffrezo J.L., Marchand N., Polo L.: Effect of measurement protocol on organic aerosol measurements of exhaust emissions from gasoline and diesel vehicles, Atmospheric Environment 140, 176-187, 2016.

Kleeman M.J., Riddle S.G., Robert M.A., Jakober C.A.: Lubricating oil and fuel contribution to particulate matter emissions from light-duty gasoline and heavy-duty diesel vehicles, Environmental Science and technology 42, 235-242, 2008.

Keyte I.J., Albinet A., Harrison R.M.: On-road traffic emissions of polycyclic aromatic hydrocarbons and their oxy- and nitri- derivative compounds measured in road tunnel environments, Science of the Total Environment 566-567,1131-142, 2016.

Kukutschová J., Roubíček V., Malachová K., Pavlíčková Z., Holuša R., Kubačková J., Mička V., MacCrimmon D., Filip P.: Wear mechanism in automotive brake materials, wear debris and its potential environmental impact, Wear 267, 807-817, 2009.

Lawrence S., Sokhi R., ravindra K.: Quantification of vehicle fleet PM_{10} particulate matter emission factors from exhaust and non-exhaust sources using tunnel measurement techniques, Environmental Pollution 210, 419-428, 2016.

Liacos J.W., Kam W., Delfino R.J., Schauer J.J., Sioutas C.: Characterization of organic, metal and trace element PM2.5 species and derivation of freeway-based emission rates in Los Angeles, CA, Science of the Total Environment 435-4365, pp. 159-166, 2012.

Lough G.C., Christensen C.G., Schauer J.J., Tortorelli J., Mani E., Lawson D.R., Clark N.N., Gabele P.A.: Development of molecular marker source profiles for emissions from on-road gasoline and diesel vehicle fleets, journal of the Air and Waste Management Association 57, 1190-1199, 2007.

Malig B. J., Green S., Basu R., and Broadwin R., 2013, Coarse particles and respiratory emergency department visits in California, Am. J. Epidemiol., 178, 58-69, doi: 10.1093/aje/kws451.

McDow S.R., Huntzicker, 1990, Vapor adsorption artefact in the sampling of organic aerosol: face velocity effects, Atmospheric environment 24A, pp 2563-2571.

Morawska L., Zhang J.: Combustion sources of particles. 1. Health relevance and source signatures, Chemosphere 49, 1045-1058, 2002.

Ntziachristos L., Gkatzoflias D., Kouridis C, Samaras Z.: COPERT: a European road transport emission inventory model. In Information Technologies in Environmental Engineering, Eds:Athanassialis I.N., Environmental Science and Engineering, Springer-verlag, Berlin Heidelberg, pp. 491-504, 2009.

Omstedt G., Bringfelt B., Johansson C.: A model for vehicle-induced non-tailpipe emissions of particles along Swedish roads, Atmospheric Environment 39, 6088-6097, 2005.

Pant P., Harrison R.M.: Estimation of the contribution of road traffic emissions to particulate matter concentrations from field measurements: A review, Atmospheric Environment 77, pp. 78-97, 2013.

Pardo M., Shafer M.M., Rudich A., Schauer J.J., Rudich Y.: Single exposure to near roadway particulate matter leads to confined inflammatory and defense responses: possible role of metals, Environmental Science and technology 49, 8777-8785, 2015.

Perrone M.G., Carbone C., Faedo D., Ferrero L., Maggioni A., Sangiorgi G., Bolzacchini E.: Exhaust emissions of polycyclic aromatic hydrocarbons, n-alkanes and phenols from vehicles coming within different European classes, Atmospheric Environment 82, 391-400, 2014.

Phuleria H. C., Geller M.D., Fine P. M., Sioutas C.: Size-resolved emissions of organic tracers from light- and heavy-duty vehicles measured in a California roadway tunnel, Environmental Science and Technology 40, 4109-4118, 2006.

Phuleria H. C., Sheesley R. J., Schauer J. J., Fine P. M., Sioutas C.: Roadside measurements of size-segregated particulate organic compounds near gasoline and diesel-dominated freeways in Los Angeles, CA, Atmospheric Environment 41, pp. 4653-4671, 2007.

Pio C., Mirante F., Oliveira C., Matos M., Caseiro A., Oliveira C., Querol X., Alves C., Martins N., Cerqueira M., Camões F., Silva H., Plana F., Size-segregated chemical composition of aerosol emissions in an urban road tunnel in Portugal, Atmospheric Environment 71, pp 15-25, 2013.

Pio C., Cerqueira M., Harrison R.., Nunes T., Mirante F., Alves C., Oliveira C., Sanchez de la Campa A., Artínaño B., Matos M.: OC/EC ratio observations in Europe : re-thinking the approach for apportionment between primary and secondary organic carbon, Atmospheric Environment 45, pp. 6121-6132, 2011.

Piot C. : Polluants atmosphériques organiques particulaires en Rhône-Alpes : caractérisation chimique et sources d'émissions, Ph.D thesis, University of Savoie-Mont Blanc, https://tel.archives-ouvertes.fr/tel-00661284, 2011.

Platt, S. M., El Haddad, I., Pieber, S. M., Zardini, A. A., Suarez-Bertoa, R., Clairotte, M., Daellenbach, K. R., Huang, R.-J., Slowik, J. G., Hellebust, S., Temime-Roussel, B., Marchand, N., de Gouw, J., Jimenez, J. L., Hayes, P. L., Robinson, A. L., Baltensperger, U., Astorga, C., Prévôt, A. S. H. : Gasoline cars produce more carbonaceous particulate matter than modern filter-equipped diesel cars, Scientific Reports 7, https://doi.org/10.1038/s41598-017-03714-9DO., 2017.

Polo-Rehn L. : Caractérisation des polluants dus au transport routier : apports méthodologiques et cas d'études en Rhône Alpes, Ph.D thesis, University of Grenoble Alpes, https://tel.archives-ouvertes.fr/tel-00876623, 2013.

Polo-Rehn L., Waked A., Charron A., Piot C., Besombes J.L., Marchand N., Guillaud G., Favez O., Jaffrezo J.L. : Estimation de la contribution des émissions véhiculaires à l'échappement et hors-échappement aux teneurs atmosphériques en PM_{10} par Positive Matrix Factorization (PMF), Pollution Atmosphérique 221, 2014.

Poprac P., Jomova K., Simunkova M., Kollar V., Rhodes C.J., Valko M.: Targeting free radicals in oxidative stress-related human diseases, Trends in Pharmacological Science 38, 592-607, 2017.

Pulles T., Denier van der Gon H., Appelman W., Verheul: Emission factors for heavy metals from diesel and petrol used in European vehicles, Atmospheric Environment 61, 641-651, 2012.

Rogge W.F., Hildemann L.M., Mazurek M.A., Cass G.R., Simoneit B.R.T.: Sources of fine organic aerosol: 2. Non-catalyst and catalyst-equipped automobiles and heavy-duty diesel trucks. Environmental Science and Technology 27, 636-651, 1993a.

Rogge W.F., Hildemann L.M., Mazurek M.A., Cass G.R., Simoneit B.R.T.: Sources of fine organic aerosol: 3. Road dust, tire debris, and organometallic brake lining dust – roads as sources and sinks. Environmental Science and Technology 27, 1892-1904, 1993b.

Sanders P. G., Xu N., Dlaka T. M., Maricq M. M.: Airborne brake wear debris: size distributions, composition, and a comparison of dynamometer and vehicle tests, Environmental Science and Technology 37, pp. 4060-4069, 2003.

Schauer J.J., Kleeman M.J., Cass G.R., Simoneit R.R.T.: Measurement of emissions from air pollution sources. 5. C1-C32 organic compounds from gasoline-powered motor vehicles, Environmental Science and Technology 36, 1169-1180, 2002.

Shirmohammadi F., Wang D., Hasheminassab S., Verma V., Schauer J. J., Shafer M. M., Sioutas C.: Oxidative potential of on-road fine particulate matter (PM2.5) measured on major freeways of Los Angeles, CA, and a 10-year comparison with earlier roadside studies, Atmospheric Environment 148, pp. 102-114, 2017.

Straffelini G., Ciudin R., Ciotti A., Gialanella S.: Present knowledge and perspectives on the role of copper in brake materials and related environmental issues: A critical assessment, Environmental Pollution 207, 211-219, 2015.

Suarez-Bertoa R., Astorga C.: Isocyanic acid and ammonia in vehicle emissions, Transportation Research Part D 49, 259-270, 2016.

Thorpe A., Harrison R.M., Boulter P.G., McCrae I.S.: Estimation of particle resuspension source strength on a major London Road, Atmospheric Environment 41, 8007-8020, 2007.

Thorpe A., Harrison R.M.: Sources and properties of non-exhaust particulate matter from road traffic: a review, The Science of the Total Environment 400, 270-282, 2008;

Timmers V.R.J.H., Achten P.A.J.: Non-exhaust PM emissions from electric vehicles, Atmospheric Environment 134, 10-17, 2016.

Tobiszewski M. and Namieśnik J.: PAH diagnostic ratios for the identification of pollution emission sources, Environmental Pollution 162, 110-119, 2012.

Turpin B.J., Saxena P., Andrews E., 2000, Measuring and simulating particulate organics in the atmosphere: problems and prospects, Atmospheric environment 34, 2983-3013.

Varrica D., Bardelli F., Dongarrà G., Tamburo E., 2013, Speciation of Sb in airborne particulate matter, vehicle brake linings, and brake pad wear residues, Atmospheric Environment 64, 18-24.

Vecchi R., Valli G., fermo P., D'Alessandro A., Piazzalunga A., Bernardoni V., 2009, Organic and inorganic sampling artefacts assessment, Atmospheric Environment 43, 1713-1720.

Von Uexküll O., Skerfving S., Doyle R., Braungart M.: Antimony in brake pads - a carcinogenic component ? Journal of Cleaner Production 13, pp 19-31, 2005.

Waked A., Favez O., Alleman L. Y., Piot C., Petit J.-E., Delaunay T., Verlinden E., Golly B., Besombes J.-L., Jaffrezo J.-L. and Leoz-Garziandia E.: Source apportionment of PM_{10} in a north-western Europe regional urban background site (Lens, France) using positive matrix factorization and including primary biogenic emissions, Atmospheric Chemistry and Physics, 14, 3325–3346, 2014.

Weber S., Uzu G., Calas A., Chevrier F., Besombes J.L., Charron A., Salameh D., Jezek I., Mocnik G., and Jaffrezo J.L., Attribution of Oxidative Potential fractions to sources of atmospheric PM. Atmospheric Chemistry and Physics, 9617-9629, 2018.

Zhang X.L., Tao S., Liu W.X., yang Y., Zuo Q., Liu S.Z.: Source diagnostics of polycyclic aromatic hydrocarbons based on species ratios: a multimedia approach, Environmental Science and technology 39, 9109-9114, 2005.

Zielinska B., Sagebiel J., McDonald J.D., Whitney K., Lawson D.R.: Emission rates and comparative chemical composition from selected in-use diesel and gasoline-fueled vehicles, Journal of the Air and Waste Management Association 54, 1138-1150, 2004.

Tables and figures

Pollutant	N_T	N_{UB}	Median increment (%)	Sign test p value	Rank Wilcoxon test p value	R with total traffic	R with HDV	R with NO_x	R with EC	Remarks
OC	57	57	22.7	0.000	0.000	0.00	0.16	0.37**	0.38**	
EC	57	57	67.8	0.000	0.000	0.50**	0.89**	0.89**	-----	R(Cu/EC)=0.83**
NO_x	55	55	73.9	0.000	0.000	0.49**	0.71**	-----	0.89**	
PM_{10}	55	55	18.7	0.000	0.000	0.33*	0.33*	0.55**	0.65**	
$PM_{2.5}$	48	48	21.3	0.000	0.000	0.38**	0.31*	0.62**	0.74**	
PM_{coarse}	48	48	8.2	0.041	0.115	0.27	0.29	0.26	0.24	
NO_3^-	48	48	28.4	0.000	0.000	0.18	0.27	0.23	0.21	
Ca^{2+}	57	26	34.2	0.011	0.005	0.42**	0.63**	0.56**	0.44**	R(Ca/Cu)=0.64**
Na^+	57	26	33.2	0.001	0.003	0.14	0.30*	0.19	0.04	
Mg^{2+}	48	48	43.1	0.000	0.000	0.24	0.29*	0.17	0.33*	$R(Mg^{2+}/NO_3^-)$=0.63**; $R(Mg^{2+}/Ti)$=0.57**
Ba	57	26	37.2	0.035	0.013	0.49**	0.26	0.25	0.35**	R(Ba/Cu)=0.57**; R(Ba/Sn)=0.74**; R(Ba/Fe)=0.71**
Co	57	26	35.6	0.003	0.000	0.15	0.07	0.00	0.04	$R(Co/SO_4^{2-})$=0.46**; R(Co/oxalates)=0.51**; $R(Co/NH_4^+)$=0.41**
Cr	57	26	86.2$	0.000	0.000	0.03	0.25	0.31*	0.40**	R(Cr/Mn=0.52**); R(Cr/Fe)=0.45**
Cu	57	26	68.9	0.000	0.000	0.67**	0.64**	0.79**	0.83**	R(Cu/Sn)=0.95**; R(Cu/Sb)=0.79**; R(Cu/Ti)=0.68**; R(Cu-An,Fla,Py, H3, H4)>0.5**
Fe	57	26	84.1	0.000	0.000	0.68**	0.60**	0.67**	0.74**	R(Cu/Fe)=0.86**; R(Fe/Sn)=0.92**
Mn	57	26	59.6	0.000	0.000	0.48**	0.66**	0.78**	0.77**	
Sb	57	26	63.3	0.000	0.000	0.44**	0.61**	0.71**	0.62**	R(Sb/Sn)=0.81**
Sn	57	26	54.1	0.000	0.000	0.71**	0.70**	0.77**	0.79**	
Sr	57	26	89.2$	0.000	0.000	0.34**	0.41**	0.31*	0.28*	
Ti	57	26	60.8	0.003	0.001	0.58**	0.59**	0.44**	0.45**	R(Ti/Al)=0.42**

Table 1a: Median increments to concentrations measured near the RN87 highway in comparison to those measured in the urban background site (given in % of total concentrations) for species for which concentrations are significantly higher at the near-traffic site according to Sign and Rank Wilcoxon tests ($p<0.05$). PM_{coarse} (difference between PM_{10} and $PM_{2.5}$) is also included in this table. R are Spearman correlation coefficients with traffic, heavy-duty traffic (HDV), nitrogen oxides (NO_x), and elemental carbon (EC). N_T: number of samples collected at the traffic site (Echirolles), N_{UB} : number of samples collected at the urban background site (Les Frênes site). $: concentrations at Les Frênes are most of the time below detection limit. * mean statistically significant at the 95% level, ** at the 99% level. Species significantly correlated with traffic indicators and for which local traffic contributions are above 50% are highlighted.

Pollutant	N_T	N_{UB}	Median increment (%)	Sign test p value	Rank Wilcoxon test p value	R with total traffic	R with HDV	R with NO_x	R with EC	Remarks
Phe (phenanthrene)	56	40	43.8	0.000	0.000	0.17	0.17	0.25	0.32*	
An (anthracene)	56	40	55.0	0.000	0.000	0.34*	0.39**	0.48**	0.51**	
Fla (fluoranthene)	56	40	70.3	0.000	0.000	0.38**	0.43**	0.51**	0.54**	
Pyr (pyrene)	56	40	81.3	0.000	0.000	0.40**	0.46**	0.50**	0.51**	
BaA (benzo(a)anthracene)	56	40	55.3	0.000	0.000	0.16	0.23	0.29*	0.39**	correlation with Levoglucosan : 0.75**
C17 (heptadecane)	56	40	78.7	0.005	0.001	-0.03	0.09	0.21	0.24	
C18 (octadecane)	56	40	39.6	0.010	0.004	0.14	0.22	0.36**	0.43**	
C19 (nonadecane)	56	40	83.1	0.000	0.000	0.23	0.29*	0.39**	0.39**	
C20 (icosane)	56	40	70.0	0.000	0.000	0.24	0.39**	0.50**	0.42**	
C21 (henicosane)	56	40	89.0	0.000	0.000	0.21	0.33*	0.46**	0.41**	
C22 (docosane)	56	40	79.3	0.000	0.000	0.27*	0.41**	0.52**	0.43**	
C23 (tricosane)	56	40	66.6	0.000	0.000	0.31*	0.40**	0.61**	0.59**	
C24 (tetracosane)	56	40	68.3	0.000	0.000	0.26	0.35*	0.50**	0.63**	
C25 (pentacosane)	56	40	48.2	0.000	0.000	0.24	0.29*	0.55**	0.61**	
C26 (hexacosane)	56	40	70.3	0.000	0.000	0.22	0.36**	0.62**	0.63**	
C27 (heptacosane)	56	40	36.4	0.000	0.000	0.17	0.18	0.36**	0.44**	
C28 (octacosane)	56	40	57.4	0.026	0.000	-0.15	-0.01	0.19	0.22	correlation with Levoglucosan : 0.55**
C29 (nonacosane)	56	40	32.0	0.006	0.000	0.15	0.16	0.24	0.26	correlation with Levoglucosan : 0.39**
C30 (triacontane)	56	40	54.7	0.002	0.000	0.03	0.16	0.33*	0.38**	correlation with Levoglucosan : 0.51**
C31 (hentriacontane)	56	40	20.4	0.007	0.003	0.14	0.21	0.35*	0.41**	correlation with Levoglucosan : 0.48**
C32 (dotriacontane)	56	40	63.4	0.004	0.002	-0.18	-0.06	0.13	0.21	correlation with Levoglucosan : 0.47**
C33 (tritriacontane)	56	40	34.4	0.030	0.008	-0.03	0.07	0.23	0.32*	correlation with Levoglucosan : 0.47**
H3 (17α21βNorhopane)	56	40	97.4$	0.000	0.000	0.29*	0.46**	0.67**	0.67**	
H4 (17α21βhopane)	56	40	97.8$	0.000	0.000	0.22	0.37**	0.59**	0.61**	

Table 1b: Median increments to concentrations measured near the RN87 highway in comparison to the urban background site (given in % of total concentrations at the traffic site) for organic species for which concentrations are significantly higher at the traffic site according to Sign and Rank Wilcoxon tests ($p<0.05$). R are Spearman correlation coefficients with traffic, heavy-duty traffic (HDV), nitrogen oxides (NO_x), and elemental carbon (EC). N_T: number of samples collected at the traffic site (Echirolles), N_{UB}: number of samples collected at the urban background site (Les Frênes site). $: concentrations at Les Frênes are most of the time below detection limit. * means statistically significant at the 95% level, ** at the 99% level. Species significantly correlated with traffic indicators and for which local traffic contributions are above 50% are highlighted.

EFs	OC	EC	NO_3^-	Na^+	Mg^{2+}	Ca^{2+}
median	16.8	39.0	1.82	0.176	0.061	1.62
IQR	8.4-27.8	35.5-45.5	0.45-2.6	0.104-0.394	0.044-0.106	0.80-2.27

Table 2a: Median emission factors for OC, EC and major ions significantly related to traffic and Interquartile Range (IQR: 25th and 75th percentiles) in mg.veh^{-1}.km^{-1}

EFs	Ba	Cr	Cu	Fe	Mn	Sb	Sn	Sr	Ti
median	66	43	300	6711	62	27	55	11	28
IQR	20-136	38-75	228-450	4527-9302	51-72	19-39	40-81	8-16	22-40

Table 2b: Median emission factors for elements significantly related to traffic and Interquartile Range (IQR: 25th and 75th percentiles) in µg.veh^{-1}.km^{-1}

EFs	Phe	An	Fla	Pyr	H3	H4
median	0.716	0.054	1.69	2.54	3.46	4.34
IQR	0.346-1.15	0.033-0.085	1.14-2.37	1.78-3.28	1.99-6.90	2.67-6.89

Table 2c: Median emission factors for PAHs significantly related to traffic and 17α21βNorhopane (H3), 17α21βhopane (H4) and their Interquartile Range (IQR: 25th and 75th percentiles) in µg.veh^{-1}.km^{-1}

EFs	C19	C20	C21	C22	C23	C24	C25	C26
median	3.6	9.5	30.3	42.5	48.0	39.9	19.8	12.7
IQR	2.0-8.3	5.2-18.9	19.9-62.4	29.8-81.4	30.6-70.3	26.1-52.5	12.5-34.2	9.3-21.9

Table 2d: Median emission factors for n-alkanes significantly related to traffic and Interquartile Range (IQR: 25th and 75th percentiles) in µg.veh^{-1}.km^{-1}

	Unit	r^2	HDV					LDV				
			Coeff.	**SD**	***p***	**conf.inter. 95%**		**Coeff.**	**SD**	***p***	**conf.inter. 95%**	
EC	$mg.veh^{-1}.km^{-1}$	0.92	148.4	22.7	0.000	102.9	193.9	30.2	1.9	0.000	26.4	34.0
Cu	$\mu g.veh^{-1}.km^{-1}$	0.73	3371	990	0.003	1312	5430	258	104	0.021	42	474
Fe	$mg.veh^{-1}.km^{-1}$	0.81	48.0	19.1	0.023	7.5	88.5	6.3	1.7	0.002	2.7	9.8
Sb	$\mu g.veh^{-1}.km^{-1}$	0.77	246	72	0.003	96	395	20.1	6.9	0.006	5.6	34.5
Sn	$\mu g.veh^{-1}.km^{-1}$	0.82	512	149	0.003	198	825	54	15	0.002	23	*85*
Pyr	$\mu g.veh^{-1}.km^{-1}$	0.60	28.4	6.3	0.000	15.6	41.1	1.459	0.658	0.034	0.121	2.798
An	$\mu g.veh^{-1}.km^{-1}$	0.55	0.435	0.128	0.002	0.174	0.697	0.0352	0.0131	0.011	0.0086	0.0618
Fla	$\mu g.veh^{-1}.km^{-1}$	0.58	7.38	3.38	0.037	0.49	14.27	1.254	0.305	0.000	0.632	1.875
C23	$\mu g.veh^{-1}.km^{-1}$	0.66	277.8	70.6	0.000	133.8	421.7	23.9	6.3	0.001	11.1	36.8
C24	$\mu g.veh^{-1}.km^{-1}$	0.62	163.9	54.0	0.005	53.7	274.1	19.2	4.8	0.000	9.3	29.0

Table 3: Results of the Multiple Linear Regressions with the heavy-duty traffic (HDV) and the light duty traffic (LDV): square correlation coefficients, unstandardized coefficients with standard deviations for HDV and LDV, p-values and confidence intervals at 95%.

	Unit	E3D		E4D		E2P		E4P		E4D+PF	
		median	IQR	median	IQR	median	IQR	median	IQR	median	IQR
EC	mg/km	31.6	29.7-41.2	27.1	15.8-37.4	<QL	<QL	0.06	0-0.06	0.37	0.12-0.44
OC	mg/km	10.7	7.3-14.4	5.6	3.3-6.0	0.3	0.2-0.4	<QL	<QL	0.14	0.07-0.18
OC/EC	-	0.29	0.24-0.33	0.16	0.12-0.19	und.	und.	und.	und.	0.61	0.40-1.94
Ba	µg/km	25.0	17.7-48.9	27.3	13.6-30.3	3. 6	2.8-5.0	-	-	0	0-0.2
Co	µg/km	<DL	<DL	<DL	<DL	<DL	<DL	-	-	<DL	<DL
Cr	µg/km	0.92	0.46-5.7	2.7	1.3-2.9	0.91	0.75-1.1	-	-	0.16	0.08-0.27
Cu	µg/km	9.2	5.2-12.9	1.1	0.56-2.4	0.40	0.33-0.79	-	-	0.14	0.10-0.29
Fe	µg/km	84	48-213	51	25-98	22	20-27	-	-	0.93	0.47-2.5
Mn	µg/km	0.56	0.49-4.3	4.2	2.4-4.3	0.42	0.13-0.81	-	-	0.07	0.03-0.09
Sb	µg/km	<DL	<DL	<DL	<DL	<DL	<DL	-	-	<DL	<DL
Sn	µg/km	0.92	0.46-5.4	2.25	1.1-2.6	0.06	0-0.14	-	-	0.06	0.03-0.08
Sr	µg/km	0.67	0.48-1.0	0.68	0.60-1.5	0.15	0.10-0.31	-	-	0.02	0.01-0.04
Ti	µg/km	8.3	7.4-10.7	15.6	12.0-28.1	2.8	1.5-4.4	-	-	<DL	0-0.1
Ca^{2+}	µg/km	<DL	0-109	39	0-52	<DL	<DL	<DL	<DL	1.2	1.0-2.8
Na^{+}	µg/km	<DL	0-89	<DL	0-60	3.6	2.7-6.0	<DL	<DL	1.5	0.34-6.8
NO_3^{-}	µg/km	226	113-267	56.5	32-352	1.7	1.3-2.3	<DL	<DL	35	26-49
Phe	µg/km	3.53	3.36-4.33	0.125	0-0.356	<QL	0-0.005	<QL	<QL	<QL	0-0.001
An	µg/km	0.091	0.07-0.11	0.013	0.01-0.02	<QL	<QL	<QL	<QL	0.015	0-0.015
Fla	µg/km	0.956	0.37-1.27	0.072	0.05-0.11	<QL	<QL	0.001	0-0.002	<QL	<QL
Pyr	µg/km	1.066	0.26-1.3	0.110	0.03-0.19	<QL	<QL	0.003	0-0.003	<QL	0-0.001
C19	µg/km	17.4	11.5-22.3	4.66	3.05-5.66	0.15	0-0.16	<QL	<QL	0.92	0-2.20
C20	µg/km	25.4	14.3-29.7	5.10	3.36-6.36	<QL	0-0.27	<QL	<QL	2.78	0.36-3.25
C21	µg/km	31.5	17.1-35.1	5.84	3.65-7.65	<QL	0-1.08	<QL	<QL	2.76	1.22-4.50
C22	µg/km	22.1	13.0-25.8	4.94	2.90-6.39	<QL	<QL	<QL	<QL	2.20	0-2.44
C23	µg/km	16.8	9.43-21.3	4.18	2.23-5.86	<QL	0-0.85	<QL	0-0.04	1.11	0-1.82
C24	µg/km	11.1	6.19-15.1	3.51	1.70-4.69	0.13	0-0.31	<QL	<QL	0.22	0-0.70
C25	µg/km	6.12	3.00-8.39	1.94	1.02-2.87	0.07	0-0.53	0.02	0.01-0.02	<QL	<QL
C26	µg/km	3.57	1.91-3.85	1.23	0.76-1.56	<QL	0-0.05	<QL	0-0.01	<QL	<QL

Table 4: Average emissions factors (median and IQR: interquartile range) determined by chassis dynamometer measurements for different types of passenger cars: Euro 3 diesel (E3D), Euro 4 diesel (E4D), Euro 2 Petrol (E2P), Euro 4 Petrol (E4P) and Euro 4 diesel equipped with particle filter (E4D+PF) using urban, urban cold, road real-driving cycles. Und: undetermined.

Ratios on	**Cu/Sb**	**Cu/Fe**	**Cu/Sn**	**Cu/Mn**	**OC/EC**
Roadside concentrations	10.4 ±4.5	0.045 ±0.015	4.7 ±1.0	3.6 ±1.6	1.00 ±0.49
Incremental concentrations	11.7 ±5.1	0.043 ±0.015	5.4 ±1.8	6.4 ±5.9	0.33 ±0.22
LDV Emission factors	12.8 ±5.2[$]	0.041 ±0.010[$]	4.8 ±1.1[$]	und.	und.
HDV Emission factors	13.7 ±4.3[$]	0.070 ±0.017[$]	6.6 ±1.1[$]	und.	und.
Traffic emission factors	12.6 ±4.7	0.046 ±0.015	5.6 ±1.8	5.7 ±2.9	0.44 ±0.32

Table 5: Ratios for road-side, incremental (road-side minus urban background) concentrations, and RN87-traffic emission factors, with standard deviations. [$]: using Taylor expansion for approx.: $var\left(\frac{x}{y}\right) = \frac{1}{\mu_y^2} var(x) + \frac{\mu_x^2}{\mu_y^4} var(y) - 2\frac{\mu_x}{\mu_x^3} Cov(x,y)$

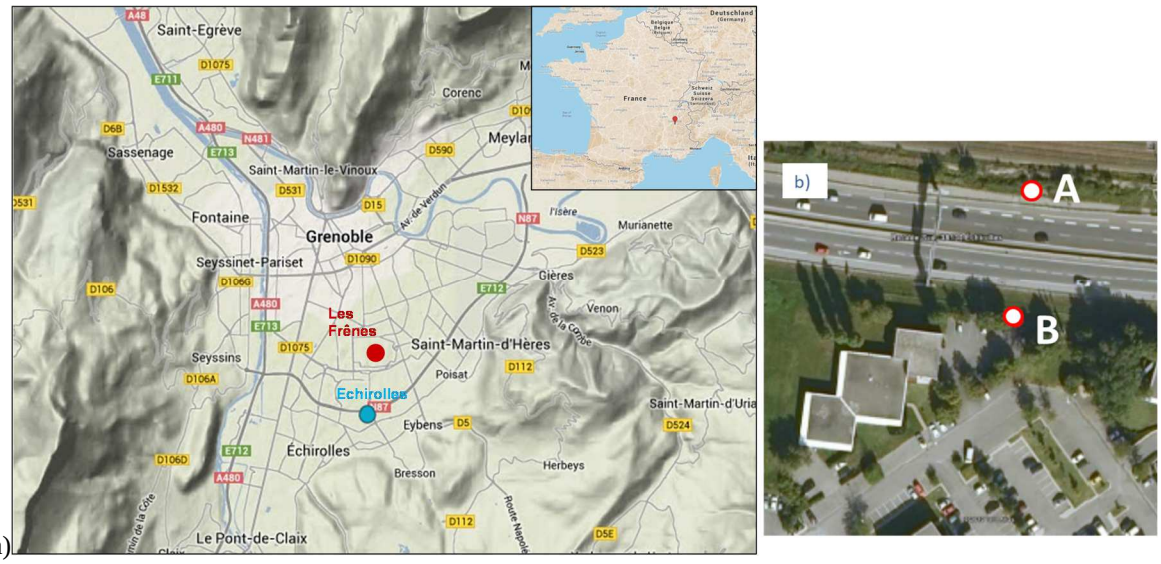

Figure 1: (a) Location of sampling sites in Grenoble-Alpes conurbation: the roadside site (Echirolles) and the urban background site (Les Frênes). (b) Echirolles sampling site: sampling and measurement devices are around the B point; the traffic electromagnetic loop monitoring are beneath the road (on the AB line), on the left, the cameras linked to automatic license plate recognition code are located on overhead gantries.

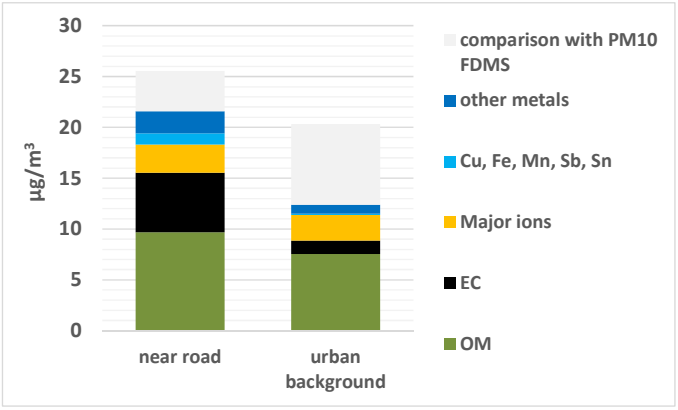

Figure 2: Median concentrations measured at the roadside site (Echirolles) and urban background site (Les Frênes) and comparison with respective median TEOM-FDMS PM_{10} concentrations. OM is computed using the factor 1.8 estimated for Grenoble city (Favez et al., 2010).

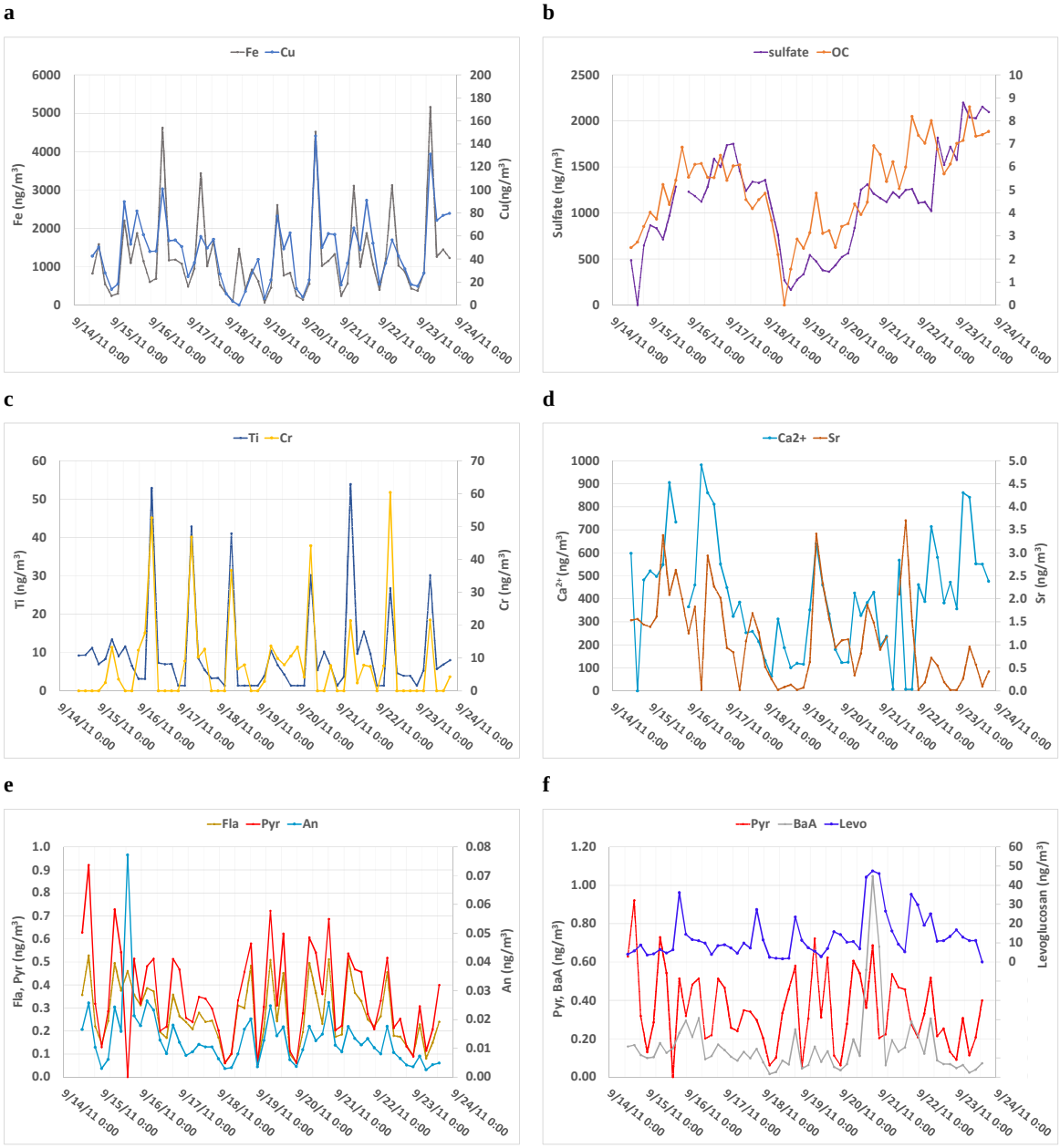

Figure 3: 4-hour concentrations measured at the traffic site: a: iron and copper; b: sulfate and organic carbon; c: chromium and titanium; d: calcium and strontium; e: fluoranthene, pyrene and anthracene; f: pyrene, benzo(a)anthracene and levoglucosan.

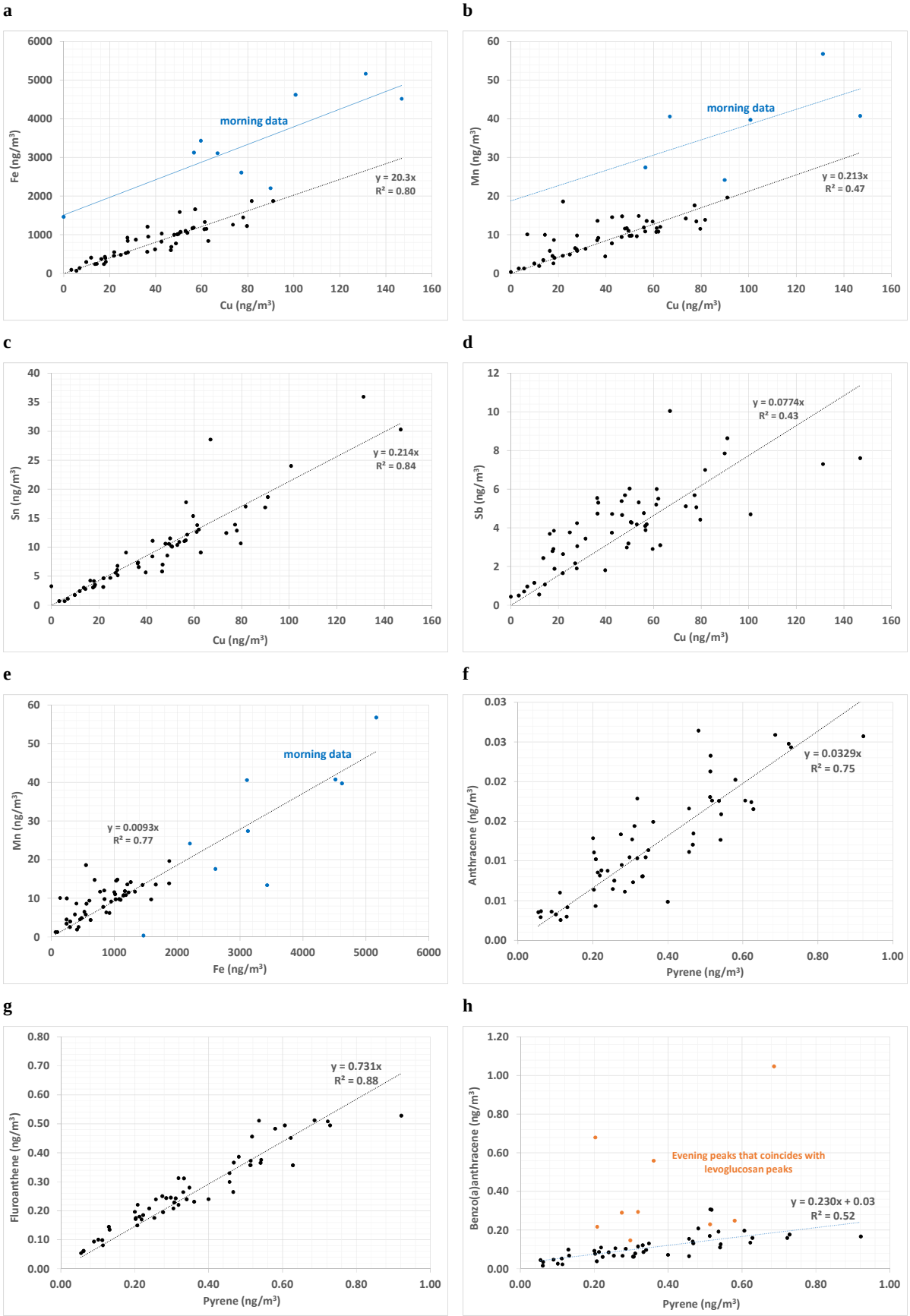

Figure 4 : Scatterplots and linear relationships for a few species : a : iron vs. copper ; b : manganese vs. copper ; c : tin vs. copper ; d : antimony vs. copper ; e : manganese vs. iron ; f : anthracene vs. Pyrene ; g : fluoranthene vs. Pyrene ; h : benzo(a)anthracene vs. pyrene

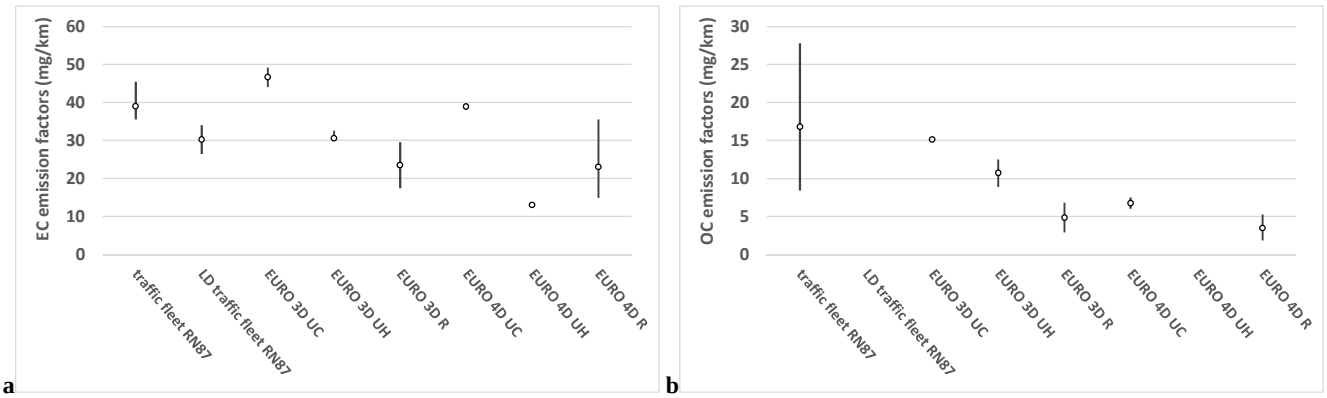

a **b**

Figure 5: Emission factors for EC (a) and OC (b) for the mixed traffic fleet and the light duty traffic of the RN87/E712 freeway and from the chassis dynamometer measurements of exhaust emissions of EURO 3 and EURO 4 vehicles for respectively urban cold (UC), urban hot (UH) and road (R) driving cycles. The emission factor for OC for the LD traffic fleet could not be determined and no data available for the hot driving conditions for the Euro 4 diesel vehicles.

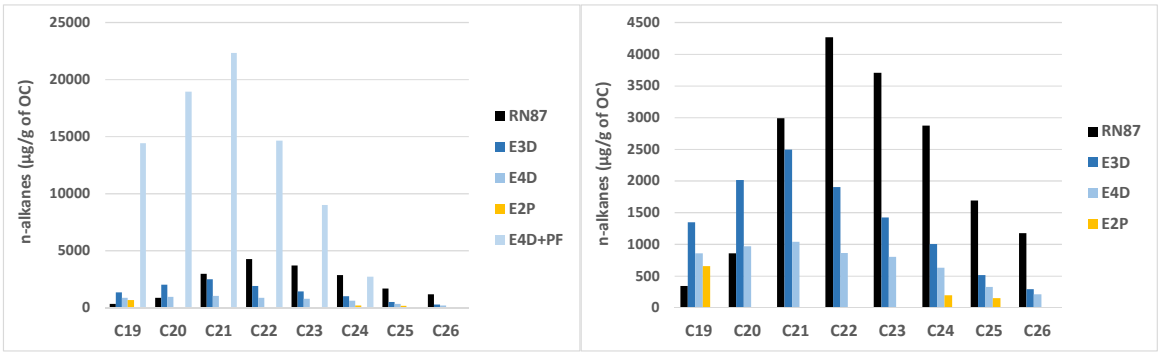

Figure 6: n-alkanes emissions normalized by OC emissions at the traffic site (RN87/E712) and from the exhaust of a Diesel Euro 3 vehicle (E3D), a Diesel Euro 4 vehicle (E4D), a Diesel Euro 4 vehicle equipped with a particle filter (E4D+PF) (on the left only) and a Euro 2 Petrol vehicles.